Marine Organic Aerosols at Mace Head: Effects from Phytoplankton and Source Region Variability

Emmanuel Chevassus[1], Kirsten N. Fossum[1], Darius Ceburnis[1], Lei Lu[1], Chunshui Lin~~Lin Chunshui~~ [1,2], Wei Xu[1a]; Colin ~~D~~ O' Dowd[1], Jurgita Ovadnevaite[1]

[1] School of Natural Sciences, Ryan Institute's Centre for Climate and Air Pollution Studies, University of Galway, Galway, Ireland

[2] Institute of Urban Environment, Chinese Academy of Sciences, Xiamen 361021

[a] Now at: State Key Laboratory of Loess and Quaternary Geology (SKLLQG), Center for Excellence in Quaternary Science and Global Change, Institute of Earth Environment, Chinese Academy of Sciences, Xi'an 710061, China

Correspondence to: Jurgita Ovadnevaite (jurgita.ovadnevaite@universityofgalway.ie)

2. Abstract

Organic aerosols (OA) are recognised as a significant component of particulate matter (PM), yet, their specific composition and sources, especially over remote areas remain elusive due to the overall scarcity of high-resolution online data. In this study, positive matrix factorisation was performed on organic aerosols mass spectra obtained from high-resolution time-of-flight aerosol mass spectrometer (HR-ToF-AMS) measurements to resolve sources contributing to ~~the~~ coastal PM. The focus was on a summertime period marked by enhanced biological productivity with prevailing pristine maritime conditions. Four OA factors were deconvolved by the source apportionment model. The analysis revealed primary marine organic aerosols (PMOA) as the predominant submicron OA at Mace Head during summertime, accounting for 42% of the total resolved mass. This was trailed by more oxidised oxygenated organic aerosols (MO-OOA) at 32%, methanesulphonic acid organic aerosols (MSA-OA) at 17%, and locally emitted peat-derived organic aerosols (Peat-OA) at 9% of the total OA mass. Elemental ratios (O:C-H:C) were derived for each of these factors: PMOA (0.66-1.16), MO-OOA (0.78-1.39), MSA-OA (0.66-1.39) and Peat-OA (0.43-1.34). The specific O:C-H:C range for MO-OOA hints at aliphatic and lignin-like compounds contributing to more oxidised organic aerosol formation. The total mass concentrations of primary organic aerosols and secondary organic aerosols were overall equal and almost exclusively present in the marine boundary layer, in agreement ~~consistently~~ with previous findings. This study reveals that OA not only reflects atmospheric chemistry and meteorology – as evidenced by the significant aging of summertime polar air masses over the North Atlantic, driven by ozonolysis under Greenland anticyclonic conditions - but also serve as indicators of marine ecosystems. This is evident from MSA-OA being notably associated with stress enzyme markers and PMOA showing the typical makeup of largely abacterial phytoplankton extracellular metabolic processes. This study also reveals distinct~~ive~~ source regions within the North Atlantic Ocean for OA factors. MSA-OA is primarily associated with the Iceland Basin, with rapid production following coccolithophore blooms (lag of 1-2 days), while diatoms contribute to a slower formation process (lag of 9 days), reflecting distinct oceanic biological processes. In contrast, PMOA is sourced from more variable ecoregions, including the Southern Celtic Sea, West European Basin, and Newfoundland Basin, with additional contributions from chlorophytes and cyanobacteria at more southerly latitudes. Overall, these findings emphasise the need for ~~further~~ longer-term investigation~~s~~ to ~~fully account for~~further map the influence of phytoplankton ~~'s~~ taxa variability ~~influence~~ on aerosol composition, and the~~ir~~ broader impacts on aerosol-climate interactions.

Keywords: Submicron Marine Aerosols, Secondary Organic Aerosols, HR-ToF-AMS, Positive Matrix Factorisation, phytoplankton

1 Introduction

The marine environment plays a critical role in Climate regulation through sea spray and gas-phase emissions from the oceans, via direct and indirect solar radiation effects and aerosol-cloud interactions governed by ocean biology, sea spray physicochemical properties and secondary reactions (Cochran et al., 2017). ~~However, a~~Aerosols in the atmospheric marine boundary layer (MBL) remain a significant source of uncertainty in radiative forcing estimates (Rosenfeld et al., 2019; Wang et al., 2020) primarily due to limited knowledge about aerosol mass, chemical composition, and particle number distributions (Carslaw et al., 2017). Radiative transfer implications from aerosol-cloud interactions alone range from -2.65 to -0.07 Wm^{-2}, contrasting with the more well-established CO_2 radiative forcing estimate of 1.83 ± 0.18 Wm^{-2} (Etminan et al., 2016). Along with this, the origin of marine organic aerosols (OA), specifically whether formed by primary or secondary processes, requires further investigation as the respective impacts from primary sea spray (Fossum et al., 2018; Ovadnevaite et al., 2011b; Xu et al., 2021) and secondary aerosols (Mayer et al., 2020; Quinn et al., 2017) on clouds formation or Atmosphere optical properties (Bian et al., 2019; Kahnert and Kanngießer, 2023; Li et al., 2023) in pristine environments is still being debated.

Primary Marine Organic Aerosols (PMOA) are part ~~consist~~ of sea spray aerosols, produced by wave breaking ~~bursting bubbles, film, jet, and spume drops~~ (Ovadnevaite et al. 2014; Veron 2015; Villermaux et al. 2022) ~~that carry sea salt particles enriched in biogenic organic aerosols~~ and made of biogenic organic matter (O'Dowd *et al*. 2004; Facchini *et al*. 2008). The majority (80 %) of fine carbonaceous particles in the clean N.E Atlantic marine atmosphere has been shown to directly originate from phytoplankton activity as reported with dual carbon isotopes analysis (Ceburnis et al., 2011)~~-~~. The phytoplankton-OA link is particularly well-established, yet the topic is still highly debated as no clear full-picture consensus has been reached owing to widely changing temporal and geographic fluctuations (Lawler et al., 2024; Lewis et al., 2021; Seidel et al., 2022). In addition, the specifics of how phytoplankton control OA chemical composition (Behrenfeld et al., 2019; Facchini et al., 2008; O'Dowd et al., 2015), particle number~~s~~ flux (Markuszewski et al., 2024; Sellegri et al., 2023), size (Croft et al., 2021; O'Dowd et al., 2004; Saliba et al., 2019), lifespan and surface tension (Lee et al., 2020; Ovadnevaite et al., 2017; Sellegri et al., 2021) are all the focus of intense ongoing investigations.

In a warming world, following a high-emissions scenario (RCP8.5) trajectory, climate change is projected to drastically alter the geographic and seasonal variability of phytoplankton blooms in the N.E Atlantic (Asch et al., 2019). Furthermore, long term trends already show that the N.E Atlantic has experienced major changes in phytoplankton functional diversity over the last 60 years (i.e. -5% dinoflagellates $decade^{-1}$ ~~whereas~~ vs ~~diatoms increased by +~~0.1% diatoms $decade^{-1}$) due to rapid warming and various environmental transformations attributable to Climate change (Bedford et al., 2020; Holland et al., 2023; Mutshinda et al., 2024). All of this strongly supports the pressing needs for further investigations on phytoplankton-aerosol interactions as environmental stressors will result in significant non-linear effects and tipping points (Ban et al., 2022; Wolf et al., 2024) .

In contrast to PMOA, marine Secondary Organics Aerosols (SOA) in the remote MBL arise from new particle formation (NPF) and are governed by other subtle chemical mechanisms. These include gas-to-particle conversion (Peltola et al., 2022; Zheng et al., 2021), oxidation of volatile organic compounds and consequent volatility reduction that leads to condensation (Hallquist et al., 2009; Kroll et al., 2018), ion-induced nucleation of biogenic particles (Kirkby et al., 2016) and fission of organic biogels (Karl et al., 2013). SOA formation occurs through various processes such as homogeneous, heterogeneous and multiple phase reactions (Marais et al., 2016; McNeill, 2015) as well photochemistry reactions (Brüggemann *et al.* 2018). While various SOA molecular classes have been identified, the complexity of SOA, which consist of thousands of multifunctional compounds (Goldstein and Galbally, 2007) including high molecular weight species and oligomers from diverse sources underscores the pressing need for continued exploration. All of this can now be partly described thanks to continuous widespread progresses in aerosol mass spectrometry (DeCarlo *et al*. 2006; Laskin, and Nizkorodov 2012).

The present study focuses on source apportionment, aiming to delineate the sources of marine OA, particularly distinguishing between SOA and PMOA sources.

Both SOA and PMOA serve as cloud condensation nuclei (CCN) (Mayer et al., 2020), impacting cloud albedo and lifetime, leading to uncertainties in global chemistry-climate models (Bellouin et al., 2020). Radiative transfer implications from such interactions range from -2.65 to -0.07 Wm-2 , contrasting with CO2 radiative forcing estimate of 1.83±0.18 Wm-2 (Etminan et al., 2016). In pristine environments, SOA nucleation events significantly shape CCN concentrations, altering cloud radiative forcing (Liu and Matsui, 2022) but so does the presence of primary sea spray (Fossum et al., 2018). Complementing this, previous literature shows that phytoplankton activity is related to emissions of organic and sulphate particle CCN precursors (O'Dowd et al., 2015; Sanchez et al., 2021). There is an ongoing debate over the respective impacts from primary sea spray (Ovadnevaite et al. 2011; King et al. 2012; Schwier et al. 2015; Xu et al. 2021) and secondary aerosols (Mayer et al., 2020; Quinn et al., 2017) on cloud formation in pristine environments. This study, thus, aims at identifying aerosol sources and quantifying elemental ratios which can serve as a proxy for ulterior parametrisations (e.g. as done in Han et al. 2022; Li et al. 2023).The present study focuses on source apportionment in a coastal environment, with the aim to separate primary OA (POA) and SOA into their respective sources. Marine SOA sources notably include methane sulphonic acid whichthat is primarily formed through the oxidation of dimethyl sulphide (Becagli et al., 2019; Hodshire et al., 2019; Mansour et al., 2024), and oxidised OAaerosols (i.e. carboxylic acids; Kawamura and Bikkina, 2016) whichthat are a complex mixtures resulting from unsaturated fatty acids oxidation found in very diverse locations (Crippa et al., 2013; Florou et al., 2024; Nøjgaard et al., 2022). On the other hand, POA sources not only include sea spray but also potential anthropogenic influences like local biomass burning (i.e. wood, peat or charcoal) or long-range continental transport (Lin et al., 2019; O'Dowd et al., 2014; Xu et al., 2020).

The source apportionment was performed with the positive matrix factorisation (PMF) model which has been widely adopted for more than two decades now (Paatero, 1999; Paatero and Tapper, 1994) and successfully used on a wide range of different instruments; HR-Tof-AMS (e.g. Aiken et al., 2008), ToF-ACSM (e.g.. Fröhlich et al., 2015), PTR-MS (e.g. Slowik et al., 2010), EESI-ToF (e.g. Tong et al., 2022), offline filters (e.g. Maykut et al., 2003), SMPS (e.g. Nursanto et al., 2023) as well as other matrix-based measurements. Several previous

remote ocean HR-ToF-AM PMF studies have been carried out in the Atlantic (Crippa et al., 2013; Huang et al., 2018), Arctic (Moschos et al., 2022; Nielsen et al., 2019; Nøjgaard et al., 2022), Mediterannean Sea (Florou et al., 2024; Mallet et al., 2019), Pacific Ocean (Loh et al., 2023, 2024) and Antarctica (Giordano et al., 2016; Paglione et al., 2024; Schmale et al., 2013) which facilitates cross-sites comparability.

~~Finally, t~~This study seeks to relate different aerosol sources and geographical regions to phytoplankton taxonomic group simulations (Rousseaux *et al.* 2013), as the effects from ocean biology ~~being currently~~are not unaccounted for in current climate models (Sellegri et al., 2021)~~., this study seeks to relate different aerosol sources and geographical regions to phytoplankton taxonomic group simulations (Rousseaux *et al.* 2013).~~ This multi-faceted approach ~~allows to place~~places the local measurements at Mace Head into the broader context of Ocean-Atmosphere interactions, allowing ~~and~~ the ~~explore~~exploration of the potential influences of marine ecosystems on atmospheric aerosols ~~loading~~ over the North Atlantic region.

2. Materials and Methods
2.1 Site Description

Mace Head (MHD) atmospheric research station is located on the west coast of Ireland (53.33°N, 9.90°W) on a peninsula exposed to open ocean air masses. These air masses, originating from a nominal clean sector (between 190° and 300°; Grigas *et al*. 2017) are predominantly steered by westerlies ushered by the polar jet's low-pressure systems. Importantly, open ocean air mases are mostly devoid of anthropogenic influences, with over 60% of air masses arriving at MHD classified as pristine marine (Grigas et al., 2017; Sanchez et al., 2022). However, the remaining 40% of all the other air masses from the 360 sector exhibit varying degrees of anthropogenic influences, particularly during or just after periods of continental outflow under high-pressure regimes (Jennings *et al*. 2003).

This study focuses on August 2015, a summertime period characterized by heightened biological activity (Behrenfeld et al., 2019) and predominant pristine marine conditions. This specific year is also marked by the onset of the *cold blob*, with the subpolar gyre region (The North Atlantic waters south of Greenland) reaching around 2°C lower than previous long-term average possibly owing to the slowing down of the Atlantic Meridional circulation and Greenland Ice melt (Rahmstorf et al., 2015; Sanders et al., 2022). As such these specific conditions could serve as an indication for future measurements of aerosols-phytoplankton interactions during cold blob phenomena.

2.2 In-situ measurements

~~Ambient submicron non-refractory aerosol major species~~Aerosol chemical composition was ~~were~~ monitored using an Aerodyne high-resolution time-of-flight aerosol mass spectrometer (HR-ToF-AMS) equipped with a standard tungsten vaporizer operated at 650°C. HR-ToF-AMS sampling covers vacuum aerodynamic size range of ~ 35 nm to ~ 1.5 µm (DeCarlo et al., 2006). The instrument working principles have been extensively described in the literature (Canagaratna et al., 2007; DeCarlo et al., 2006). The HR-ToF-AMS used a 5 min time resolution scan on the single-reflection highly sensitive V mode configuration (mass resolution up to 3000 m/Δm) while detection limits were estimated based on the approach described by Drewnick *et al* (2009). Ionisation efficiency (IE), particle velocity and inlet flow were determined following standard methods while applying standard relative ~~R~~IE (RIE) for species (Nault et al., 2023; Xu et al., 2018). The particle transmission and detection efficiency expressed as the collection efficiency (CE; Huffman *et al*. 2005) was corrected for

detection losses due to particle bounce and lens efficiency by applying the composition-dependent collection efficiency (Middlebrook *et al*. 2012)..

The AMS data were analysed using SQUIRREL (SeQUential Igor data RetRiEvaL) v1.65B and PIKA (Peak Integration by Key Analysis) v1.25B software packages. Sea salt was estimated based on a scaling factor of 51 of the common sea salt ion NaCl⁺ (m/z 57.96) (Ovadnevaite et al. 2012) while MSA was quantified by upscaling the CH_3SO_2 (m/z 79) ion (Ovadnevaite *et al*., 2014). Interferences from MSA on SO_4 and OA were accounted for as follows:

$$SO_{4\ corrected} = SO_4 - \frac{CH_3SO_2 * 12.48}{RIE_{SO_4}}$$

$$OA_{\ corrected} = OA - \frac{CH_3SO_2 * 15.86}{RIE_{Orgs}}$$

An improved Ambient (I-A) method was adopted for the mass spectra elemental ratio analysis of O:C, H:C, N:C, S:C, and the OM:OC (organic matter to organic carbon) ratio (Canagaratna et al., 2015). High-resolution analysis was performed on each m/z in the mass range 12–130 m/z with ion fitting applied to difference between open and closed spectra. Based on their elemental composition (C, O, H, N, S), ions were then grouped into chemical families: C_x, C_xH_y, $C_xH_yO_z$ (z = 1), $C_xH_yO_z$ (z > 1), $C_xH_yN_w$ (w = 1), $C_xH_yN_w$ (w >1), C_xS_j, H_yO_z, N_wH_y, N_wO_z, S_jO_z, and C_xS_i where the indices x, y, z, w, j represent the number of C, H, O, N, S atoms, respectively.

The concentration of equivalent black carbon (eBC) was measured by a multi-angle absorption photometer (MAAP, Thermo Fisher Scientific model 5012). The MAAP operated at a flow rate of 10 L min⁻¹ and a 5 min time resolution. The transmittance and reflectance of eBC-containing particles were measured by the MAAP at two different angles to derive optical absorbance as detailed in (Xu et al., 2020).

Carbon monoxide (CO) measurements were also conducted using a model RGA-3 CO analyser (Trace Analytical, Inc., CA, USA), which operates on the principle of hot mercuric oxide reduction gas chromatography (Derwent et al. 1994).

Ozone (O_3) was measured at the station with an UV O_3 spectrometer (Model 8810, Monitor Labs San Diego, CA), the raw voltage output was converted to concentration values based on Automatic Urban/Rural Network (AURN) calibration audits (Derwent *et al*. 2018). Finally, meteorological data were continuously recorded at the station (including rainfall, irradiance<s>solar radiation</s>, wind speed, wind direction, temperature, relative humidity and pressure) using standard meteorological instruments and retrieved using the *worldMet* R package (station ID: 039630-99999) from the NOAA ISD website (https://www.ncdc.noaa.gov/isd).

2.3 Source apportionment

The HR organic mass spectra was deconvolved using the Positive Matrix Factorisation (PMF; Paatero and Tapper 1994; Paatero 1999) source-receptor model to investigate the various source contributions to OA. A major advantage of using HR data over unit mass resolution (i.e. ToF-ACSM studies) is the distinct differentiation of multiple ions sharing the same nominal mass, thereby allowing for a more exact characterisation of the temporal fluctuations of different ion families (e.g., $C_xH_y^+$, $C_xH_yO_z^+$). The information richness in the HR-ToF-AMS datasets, as a result of the improved chemical resolution, is advantageous for

restricting the PMF solutions, minimising rotational ambiguity and results in more reliable solutions and a larger number of interpretable OA factors.

The IGOR PRO Source Finder (SoFi v6.8.1) toolkit (Canonaco *et al*. 2013) was used to run the PMF algorithm. Solutions were assessed across 2 to 12 factors using the unconstrained factors rotational Fpeak tool. Factors were explored for Fpeaks (rotations) between −1 and 1 (0.1 steps). A final solution consisting of 4 factors was retained as the optimal solution based on several considerations. These include its Q/Qexp ratio value (1.38),which is tested for a range of FPEAKS and scaled residuals distribution (as recommended by Zhang *et al*. 2011). The solutions were also investigated in regard to key diagnostic plots, diurnal profiles, correlations with meaningful external tracer time series and reference mass spectra (Canonaco et al. 2021) extracted from the aerosol mass spectrometer database (Ulbrich et al., 2009).

2.4 Air masses trajectory analysis

Air masses back trajectories analysis was performed using the Hybrid Single Particle Lagrangian Integrated Trajectory (HYSPLIT) (Stein et al., 2015). Meteorological data were accessed from the Global Data Assimilation System (GDAS) archived by NOAA Air Resources Laboratory. HYSPLIT was used to calculate 72-hours back trajectories every 3 hours with arrival starting height set to 100m above ground level. To investigate potential source regions leading to total particle mass concentrations from each resolved source, the back trajectories were gridded to $1° × 1°$ grid cells and linked to particle concentrations using trajectory source contribution functions. While common source contribution functions assume that trajectories centrelines are accurate, we focused instead on the Simplified Quantitative Transport Bias Analysis (STQBA) method which considers plumes transport bias along air mass trajectories as a more robust approach.

The Boundary layer height (BLH) was determined from the fifth generation ECMWF (European Centre for Medium-Range Weather Forecasts) atmospheric reanalysis (ERA5) dataset based on the bulk Richardson number (Guo et al., 2021) by mapping HYSPLIT trajectories footprint along the gridded BLH data. This was used to find the fraction of time spent over the Ocean, within the Marine Boundary Layer (MBL; altitude <BLH), in the Marine Free Troposphere (MFT; altitude >BLH) and in the planetary boundary layer over land (PBL; altitude < BLH). The R package *rnaturalearth* was also used to obtain a high-resolution land mask for Ireland allowing for identification of purely marine air masses (no advection over land for at least 3 days prior to being sampled at MHD) and aided in delineating lands from oceans.

Finally, NASA Ocean Biogeochemical Model (NOBM) taxonomic group simulations (Rousseaux *et al*., 2013) for *coccolithophores*, *diatoms*, *chlorophytes* and *cyanobacteria* were used to visualise phytoplankton geographic repartition estimates as well as for lags calculations with OA similarly to O'Dowd *et al* (2015).

2.5 Transfer entropy analysis

The R package RTransferEntropy (Behrendt et al., 2019) was used to quantify the information flow between time series using the transfer entropy (TE) as previously done on recent SOA studies (Long et al., 2023; Sinha et al., 2024). Transfer entropy (TE) is a prediction model that quantifies the directional influence between two time series X and Y by determining how the past values of one series predict the future behaviour of the other (Schreiber, 2000). TE is calculated using Rényi entropy, a generalisation of Shannon entropy that offers enhanced robustness in the presence of tails effects. To account for spurious information transfer, the transfer entropy is also estimated from a shuffled version of the time series. This shuffled estimate called effective

235 transfer entropy (eTE) is used to correct for sampling bias, ensuring the validity of the results. Statistical significance is assessed with a bootstrapped Markov chain, where a p-value of less than 0.05 indicates a significant information transfer between X and Y. The reader is referred back to (Behrendt et al., 2019) for more details.

3. Results

240 **3.1 Submicron aerosol chemical composition overview**

The mass concentration time series of organic aerosols (OA), methane sulphonic acid (MSA), sulfate (SO_4^{2-}), nitrate (NO_3^-), ammonium (NH_4^+) and sea salt measured by the HR-ToF-AMS as well as eBC from MAAP measurements are shown on Figure 1. The average chemical composition was dominated by OA (32%), followed by SO_4^{2-} (31%), sea salt (20%), MSA (7%), NH_4^+ (6%), NO_3^- (2%) and eBC (2%) (Figure 1).
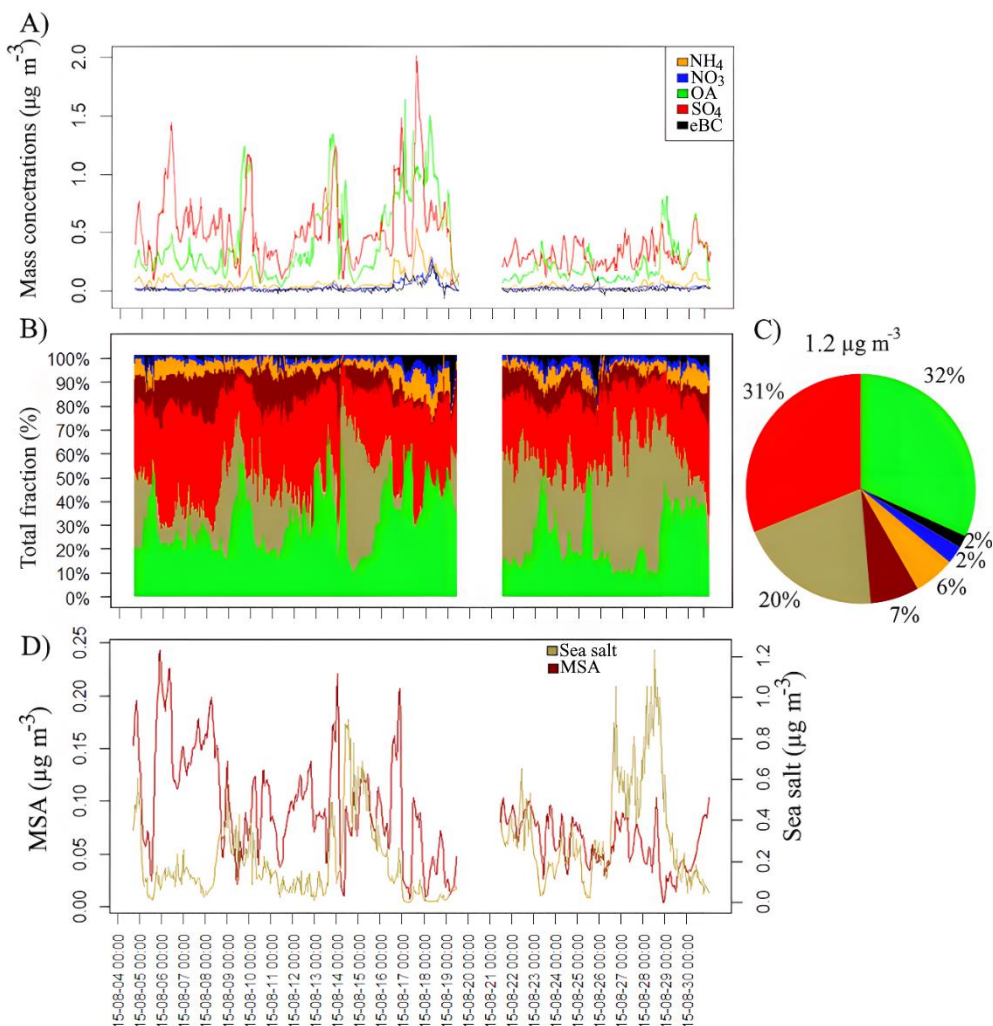
245

Figure 1. A) OA, SO₄., NH₄, NO₃ and eBC mass concentrations time series – µg m⁻³ B) Relative contributions to total PM1 C) Pie plot of total contributions to total PM1 D) shows MSA and sea salt – µg m⁻³.

The total average bulk submicron aerosol mass was 1.2 µg m^{-3} over the entire measurement period. These high

250 SO_4^{2-} and OA relative contributions and overall low concentrations are common for coastal sites during summertime in the marine boundary layer as reported over the North & South Atlantic Ocean (Huang et al., 2018; Ovadnevaite et al., 2014b) as well as in the Artic (Nielsen et al., 2019; Willis et al., 2017). MSA in

particular showed mass concentrations values of 0.08 ± 0.04 µg m^{-3} in the range of those previously reported at Mace Head (0.05 ± 0.04) (Ovadnevaite et al., 2011a) and more diverse locations such as the central Arctic (Dada et al., 2022) and the Atlantic Ocean from 53° N to 53° S where average mass concentrations of 0.04 ± 0.03 µg m^{-3} (Huang et al., 2018) were reported.

The low mass concentrations of NH_4^+, NO_3^- and corresponding N:C ratio of 0.006 ± 0.002 (Figure S1), indicate a limited presence of amino acids (below detection limit) from usual sources such as the North Atlantic oligotrophic gyre, ornithogenic emissions (i.e., birds), phytoplankton, bacteria, or in situ atmospheric processes (van Pinxteren et al., 2022; Schmale et al., 2013).

Following eBC thresholds established for the North-East Atlantic (Grigas et al., 2017), pristine conditions (eBC levels below 0.015 µg m^{-3}) were observed during 60.4% of the measurement period. Clean conditions (eBC levels between 0.015 and 0.05 µg m^{-3}) prevailed for 30.5% of the time, and moderately polluted conditions (eBC levels between 0.05 and 0.3 µg m^{-3}) occurred for 9.1% of the time with a significant pollution event spanning from August 17th to 19th 2015 onwards.

Likewise, CO mixing ratios were below 100 ppb for over 70% of the time, similarly to other pristine sites (Zhao et al., 2022). Winds advected through the clean sector (190-300°) for over 78% of the time. Finally mean wind speed was 6.6 ± 3.1 ms^{-1} exceeding the whitecap threshold of 4 m s^{-1} (O'Dowd et al., 2014) for 77% of the time, hinting at strong- sea spray influences.

There were also SOA influences were also consequent as revealedindicated by with the average OM/OC (organic matter to organic carbon ratio) value of 2.10 ± 0.14 (Figure S1), aligning with the value of 1.9 previously reported for clean aged marine polar air masses at MHD (Ovadnevaite et al. 2014). Additionally, AMS derived OM/OC values in the high Arctic (Nielsen et al., 2019) also fall within the range of 1.96 to 2.42 for PMOA (primary marine organic aerosols) and MO-OOA (more oxidised organic aerosols) respectively, here median OM/OC value was 2.11 with minimum and maximum OM/OC values of 1.71 and 2.42 respectively. This indicates the presence of both POA (i.e., saturated hydrocarbons, unsaturated hydrocarbons and cycloalkanes) as well oxygenated SOA formed with photochemical processing during long range transport (Aiken et al., 2008; Simon et al., 2011).

To get a better sense of the aerosol sources, the respective contributions of the marine boundary layer (MBL), marine free troposphere (MFT) and boundary layer over land (BL) are shown in Figure S2. Overall, the measurement period was dominated by marine boundary layer influences (91% of the time), with minimal marine free troposphere influences (8%) and extremely low land-influences from the planetary boundary layer (1%) further hinting atevidencing pristine marine conditions.

3.2 Source apportionment

To accurately classify and categorise the diverse sources of OA that are present at Mace Head, source apportionment was performed utilising the Positive Matrix Factorization (PMF) method on the organic mass spectrum, which ranged from m/z 12 to m/z 130. The resulting chosen four-factors solution, as depicted in Figure 2, yielded a Q/Qexp ratio of 1.38 and accounted for up to 90% of the total OA mass. Solutions with a

higher number of factors introduced splitting and did not show additional emergent interpretable sources (Figure
290   S3, Text S1).

The following four factors, namely Methane Sulphonic Acid, More Oxidised Organics, Primary Marine
Organics and Peat, were determined as the optimal representation of the aerosols at Mace Head:

Methane Sulphonic Acid Organic Aerosols (MSA-OA):), Representing representing approximately 17.2% of
the total OA mass, MSA displayed a distinct m/z fragment at m/z 78.98 ($CH_3SO_2^+$), accounting for 36.3% of its
295   total mass spectra signal intensity. The identification of specific methane sulphonic acid tracer ions further
substantiated its origin. More details on all factors are provided below in sections 3.2.1-3.2.4.

More Oxidised Organic Aerosols (MO-OOA): Making up about 31.8% of the total elucidated PMF solutions,
this factor exhibited prominent m/z fragments at m/z 27.99 and m/z 43.99 and showed significant correlations
with reference mass spectra for MO-OOA (R = 0.97) (Hu et al., 2015), SV-OOA (R = 0.76) (Mohr et al., 2012),
300   and was interpreted as MO-OOA after examining elemental ratios and correlations.

Primary Marine Organic Aerosols (PMOA): Comprising roughly 42.2% of the total resolved PMF solutions.
This factor exhibited m/z fragments similar to MO-OOA (Schmale et al., 2013), but with higher contributions
from aliphatics (C_xH_y) such as alkyls (dominant in sea spray during phytoplankton blooms; Cavalli et al. 2004),
alkenes (i.e. phenols or humic materials; Bahadur et al. 2010) and functional derivatives such as alcohols
305   ($C_xH_yO_z$, where z=1) as established in earlier studies (Ovadnevaite et al. 2011; Crippa et al. 2013).

Peat-OA: accounting for approximately 8.8% of the total PMF solutions, was characterised by saturated
hydrocarbons (C_xH_{2y+1}), unsaturated hydrocarbons (C_xH_{2y-1}) and cycloalkanes (C_xH_{2y}) ion series. This factor
was identified as Peat-OA owing to its good correlation (R=0.75) with the Peat-OA reference mass spectra (Lin
et al., 2017). Additionally, its mass spectrum was marked by cellulose pyrolysis fragments typical for
310   levoglucosan (i.e. $C_2H_4O_2^+$ at m/z 60 and $C_3H_5O_2^+$ at m/z 73) and by the dominance of $C_3H_7^+$ rather than $C_2H_3O^+$
at m/z 43 which facilitated the distinction of peat emissions over wood or smoky coal emissions.
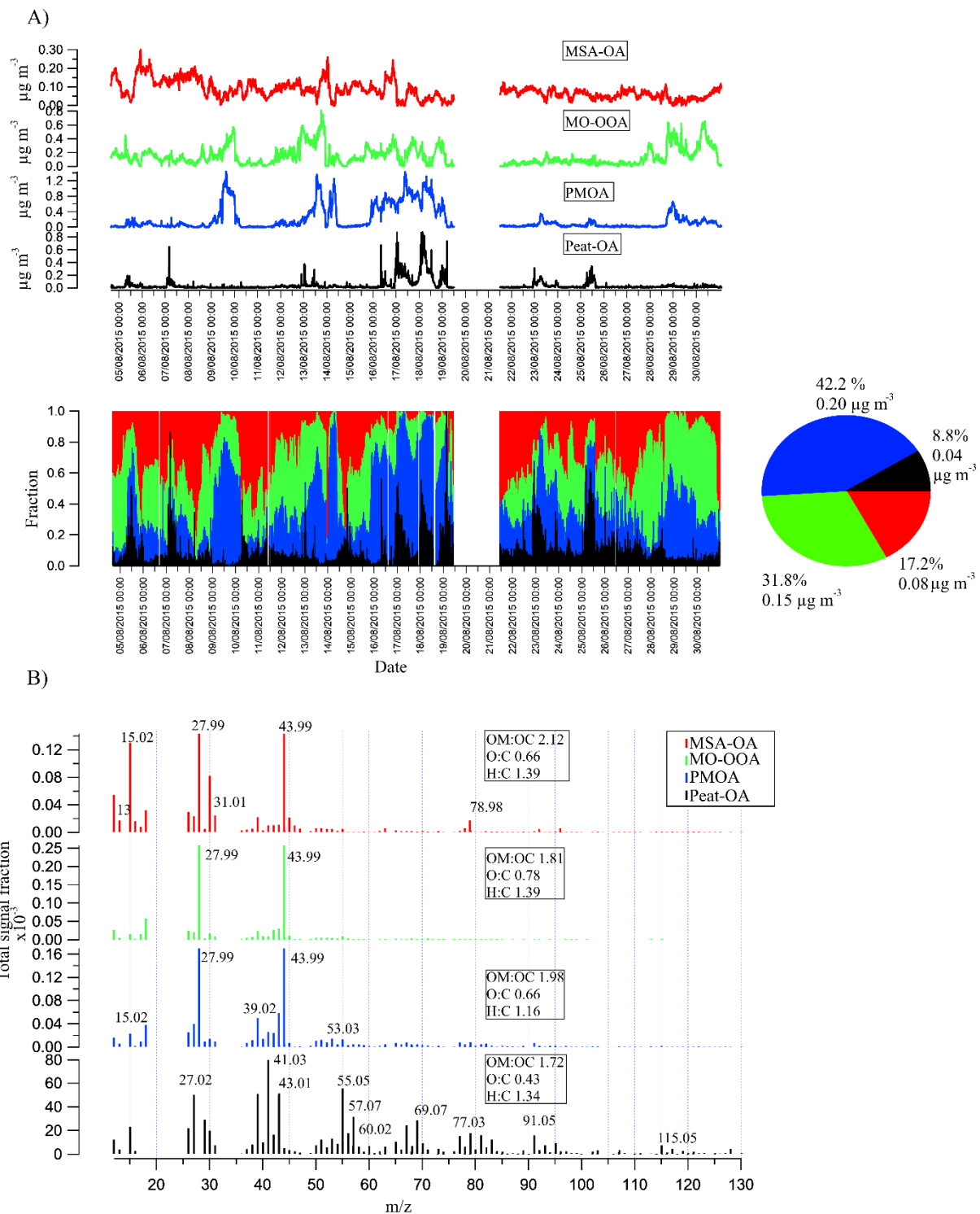
Figure 2. A) Factors time series (MSA-OA in red, MO-OOA in green, PMOA in blue, Peat-OA in black) and associated relative contribution time series and pie chart showing fractions and respective mass concentrations (μg m⁻³) for the whole period B) Factors mass spectra (MSA-OA in red, MO-OOA in green, PMOA in blue, Peat-OA in black) and associated improved ambient OM:OC, O:C and H:C ratios (Canagaratna et al., 2015).

3.2.1 More Oxidised Oxygenated Organic Aerosols (MO-OOA)

MO-OOA main contributing ions are associated with oxygenated compounds belonging to the COOH functional group (Figure S5), reflecting pronounced fragmentation of mono- and dicarboxylic acids into fragments with multiple oxygen atoms (Duplissy et al., 2011). Specifically, $C_xH_yO_z$ (z > 1) ions family accounts for 63.1% of the total mass spectra intensity, followed by $C_xH_yO_z$ (z = 1) ions family (m/z 27.99, m/z 43.02, m/z 42.01…) contributing 13.68% to MO-OOA, adding up to a total contribution of 76.8%. Additionally, CO^+ and CO_2^+ each accounts for 25% of MO-OOA intensity which is typical for remote Ocean carboxylic acids (Dominutti et al., 2022).

In contrast, C_xH_y (aliphatics) ions family (m/z 13.00, m/z 15.02, m/z 16.03…) contributes only 13.7% to MO-OOA total mass spectra intensity. Nitrogen-containing ions fragments constituted a very low portion of the signal (0.8%), similarly to previous remote ocean measurements (Ovadnevaite et al. 2011). The weak contribution from $C_2H_3O^+$ (3.16%) which has been reported to be predominantly due to non-acid oxygenates (Ng *et al*., 2011a) suggests a considerable prevalence of aging/oxidation during transport over the North-East Atlantic Ocean. This is also further confirmed by the low m/z 43:44 ratio of 0.12 hinting to MO-OOA rather than less oxidised species (Ng et al., 2011). This factor respective O:C ratio and H:C ratio of 0.78 and 1.17 further agree with MO-OOA reported at other similar locations (Figure S4). MO-OOA also has a strong contribution from CO_2^+ (25.7%) which is assumed to originate mainly from acids or acid-derived compounds (Duplissy et al., 2011; Ng et al., 2011) that are known to be mostly water-soluble (Decesari et al., 2007) such as organic acids (e.g., mesotartaric acid, meso-erythritol, tartaric acid, oxalic acid) formed from oligomerization of small α-dicarbonyls (e.g., glyoxal) (Cui et al., 2022).

MO-OOA formation through ozonolysis is postulated based on a robust hourly averaged correlation (R=0.67) of MO-OOA to O_3 across the entire observational period (Figure S6-B). Using the effective transfer entropy test (Behrendt et al., 2019) further reveals the non-linear dynamics between O_3 and MO-OOA, indicating O_3 as a significant reactant in the formation of MO-OOA from its precursors with a transfer entropy value (Figure 3) of 0.0144 and an effective transfer entropy value of 0.0127 ± 0.0009 (p-value<0.05). In other words, there is a significant directional information flow between the two time series. Figure 3 also shows that MO-OOA is a mix of local (Peat-OA) and regional marine influence (PMOA, but also MSA-OA to a lesser extent) all eventually concurring to MO-OOA formation, with ozone contributing 3x more information to MO-OOA than irradiance does. Although, irradiance and ozone was measured onsite and may not be as directly related to conditions of aerosol during transport. This Yet, this finding aligns with studies showing O_3 to be a strong oxidation driver during summertime in the marine environment (Ovadnevaite *et al*., 2011), where unsaturated aliphatic chains (C=C double bonds) react with ozone to form oxidised compounds (Decesari *et al*, 2011).
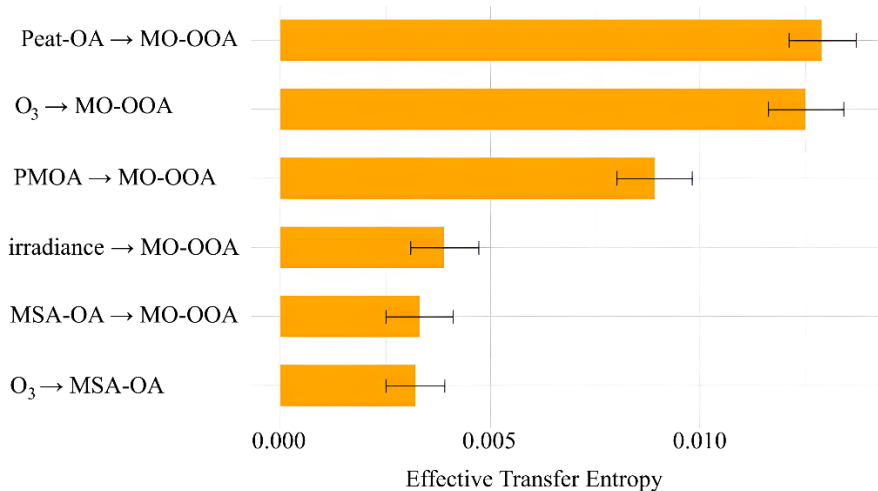
Figure 3. Significant (p-value=0) effective transfer entropy flow values between PMF factors, ozone and irradiance.

3.2.2 Methanesulphonic Acid Organic Aerosols (MSA-OA)

The mass profile of MSA-OA reveals that two oxygenated carbon families CHO (sum of $C_xH_yO_k$ and $C_xH_yO_w$ where k = 1 and w > 1) dominate 53.4% of the total mass spectra fraction followed by aliphatics (pure Hydrocarbon-like, $C_xH_y^+$) whose fraction accounts for 33.3% (Figure S5). MSA-OA is clearly identified owing to its substantial contribution from the $C_xS_y^+$ family (6%) over other sources, this is in line with the $C_xS_y^+$ contribution (7%) for MSA-OA also reported by Huang *et al.* (2018). The excellent correlation (R=0.82) between this factor and the $C_xS_y^+$ family (Figure S6-D) also further highlights the organosulphurs nature of MSA-OA as opposed to other factors.

Similarly, to results reported by Schmale *et al.* (2013), the correlation coefficient with the AMS database MSA-OA laboratory reference spectrum (Figure S6-A) is rather moderate (R=0.55), although this factor spectra still allows for the precise identification of characteristic MSA ions at m/z 44.98 (CHS^+), 47.00 (CH_3S^+), 64.97 (HSO_2^+), 77.98 ($CH_2SO_2^+$), 77.99 ($CH_3SO_2^+$), and 95.99 ($CH_4SO_3^+$). MSA-OA O:C and H:C ratios were 0.66 and 1.39 respectively, close to values (O:C: 0.54, H:C: 1.42) reported by Loh *et al.* (2022).

MSA-OA C_xH_y family also features a typical CH_3^+ ion at m/z 15.02 that is absent from other factors. Similarly, the $C_xH_yO_w$ (w=1) family features the tracers ions CH_2O^+ (8.2%) and CH_3O^+ (2.4%) which are heat stress related marker (Faiola et al. 2015) attributed to methyl jasmonate (MeJA) and possibly acrylic acid (Van Alstyne and Houser, 2003) or other oxylipins stress enzymes (Aguilera et al., 2022; Koteska et al., 2022) which are known to be emitted by kelp (Saha and Fink, 2022) or phytoplankton species (Koteska et al., 2022).

The $C_xS_y^+$ fragment family was dominated by CHS^+(25.9%), $CH_3SO_2^+$ (20.2%), CH_2S^+ (12.2%), $CH_4SO_3^+$ (7.5%), CH_3SO^+ (7.2%), $CH_2SO_2^+$, (6.9%), $CH_4SO_2^+$ (5.45), CH_3S^+ (6.41%), $C_2H_4SO_2$ (5.4%) and CH_2SO^+ (2.5%) which are common MSA ions found in the literature (Moschos et al., 2022). Overall, the $C_xH_y^+$ and $C_xS_y^+$ fragment ions families indicate a clear MSA fragmentation pattern with a characteristic high CH_3^+ relative intensity (13%) typical for marine SOA in line with recent findings (Huang et al., 2018; Moschos et al., 2022).

Finally, MSA-OA correlated moderately (Figure S6-B) with particulate sulphate (R=0.51) which is expected since dimethyl sulphide, released by phytoplankton, can be oxidized to either form MSA or sulphur dioxide and then to sulphuric acid, leading to their partitioning into the particulate phase (Mungall *et al*, 2018). Although MSA is often found in clusters with amine, dimethylamine or trimethylamine (Bork et al., 2014; Chen et al., 2016; Paglione et al., 2024), the MSA spectrum minor methylamine contributions such as m/z 30 (CH_4N^+), m/z 41 ($C_3H_5^+$), m/z 42 ($C_2H_4N^+$) (Malloy et al., 2009) were too sparse to assume involvement.

3.2.3 Primary Marine Organic Aerosols (PMOA)

High-resolution mass spectrum of this factor reveals that two CHO oxygenated carbon families (sum of $C_xH_yO_k$ and $C_xH_yO_w$ where x = 1 and w > 1) dominate 61.5% of the total mass spectra followed by aliphatics (pure Hydrocarbon-like, C_xH_y) whose fraction accounts for 36.2% of the total mass spectra signal (Figure S5) aligning with previous findings reported by Ovadnevaite *et al* (2011). The $C_xH_yO_w$ (w=1) family features ions series (m/z 55.02, 69.03, 83.05, etc…) related to alkenyl groups, diunsaturates, cyclic alcohols, and ethers. Such functional groups repartition is consistent with previous reports of water-insoluble organics being formed in sea spray (O'Dowd *et al*. 2004; Ovadnevaite *et al*. 2011). Additionally, this factor mass spectrum closely resembles (R=0.99) marine organic aerosols (MOA) mass spectra (Ovadnevaite *et al*. 2011) (Figure S6-A) and its O:C ratio of 0.66 and an H:C ratio of 1.16 respectively are close to literature O:C values for sea spray (Ovadnevaite *et al*. 2011; Flerus *et al*. 2012; Willoughby *et al* 2016) (Figure S4).

PMOA C_xH_y mass spectra family is dominated by ion series C_xH_{2y-3} (m/z 39.02, 53.03, 67.05 etc…) indicating dienes, alkynes, and cycloalkenes contributions, which is further confirmed by the presence of C_xH_{2y-1} ions series (m/z 27.02, 41.04, 55.05 etc…) while the C_xH_{2y+1} family (m/z 43.05, 57.07, 83.08 etc... y>2) indicative for anthropogenically influenced refined hydrocarbons is absent from this factor mass spectra. The marine biogenic origin of this factor is also indicated by the absence of alkanes (C_xH_{y+2}; m/z 16.03, 58.08, 72.09) which are typical for continental air masses (Lewis et al., 2021) and by its lack of correlation with eBC (R=0.17) thereby excluding contribution from fossil hydrocarbons to PMOA. The C_xH_y family is also marked by alkyls (C_xH_{2y+1} ;m/z 15.02, 29.03, 37.00 etc…) which have been reported to be dominant in sea spray during phytoplankton blooms as a possible result of phosphate cycling (Cavalli, 2004; Meador et al., 2017).

Prior atmospheric measurements have shown that PMOA containing a large fraction of alkenes and oxygenated functional groups (ie. alcohols, ethers, aldehydes, ketones) are dominated by insoluble organic colloids and aggregates (Facchini et al., 2008; Rinaldi et al., 2020) composed of microgels derived from phytoplankton extracellular metabolic extraction and adsorption organic pool rather than exopolymers produced from bacteria, with abacterial microgels aerosols being quite common and possibly accounting for 50-90% or phytoplankton derived organics (Bigg and Leck 2008; Bates et al. 2012; Liu et al. 2023). These bacterial exopolymers would follow the makeup of ordinary bacterial cell fragments, which comprise approximately 55% nitrogen-containing organics and 10% carbohydrates (Schmale et al., 2013). The latter are accounted for by summing up pure carbohydrates (i.e.; glucose, saccharose, mannitol and glycogen) identified by typical fragments (Schmale et al., 2013; Schneider et al., 2011) at m/z 56.03 ($C_3H_4O^+$), m/z 60.02 ($C_2H_4O^+$), m/z 61.03 ($C_2H_5O^+$) and m/z 85.03 (C_4H_5O+) only amounting for about 1.3% of the total PMOA aerosols mass. Similarly, contributions from other bacterial tracers such as glycogen; m/z 55.01 (1.36%), mannitol; m/z 56.02 (0.4%) and polysaccharide species; m/z 97.02 ($C_5H_5O_2^+$) and m/z 125.02 ($C_6H_5O_3^+$) (Glicker et al., 2022) tracer ions were also relatively poor

(0.7%). All of this paired with below detection limit amino acids thus implicates that PMOA organic pool was largely shaped by abacterial processes. However, bacterial influence cannot be ruled out entirely as carbohydrates might have been processed by enzymes or acidity during air masses transport and subsequent aging (Zeppenfeld et al., 2023). A potential important tracer for this activity could be lactic acid which has been observed before in sea spray owing to microorganisms fermenting sugars (Miyazaki et al., 2014; Paglione et al., 2024), although lactic acid itself still remains understudied in HR-ToF-AMS studies.

3.2.4 Peat Related Organic Aerosols (Peat-OA)

Although the measurement period is largely dominated by pristine ocean air masses, some residential heating influence is still observed owing to local peat burning. Peat-OA mass spectra is largely dominated by saturated Alkanes-$C_xH_{2y+1}^+$ (76.92%) and Alkenes-$C_xH_{2y-1}^+$ (Figure S5) which is typical for peat. This factor mass spectrum correlates well (R=0.86) with previous measurements of Peat-OA in Galway city (Lin et al., 2017) (Figure S6-A). More specifically, the presence of aromatic ion series at m/z 77.03 ($C_6H_5^+$) and m/z 91.0.5 ($C_7H_7^+$) (Cubison et al., 2011) and the ratio between m/z 55.05 ($C_4H_7^+$) and m/z 57.07 ($C_4H_9^+$) of 1.74 as well as the ratio between m/z 43.05 ($C_3H_7^+$) and m/z 44.01 ($C_2H_3O^+$) of 1.03 all allow for the clear distinction of peat burning over other sources (Lin et al., 2017). Peat-OA was freshly emitted as evidence by the pollution wind rose (Figure S7-E, S7- F) and concurrent increase along with eBC (R=0.72) indicate that both were locally co-emitted within the PBL.

3.3 Elemental ratios -Van Krevelen diagram

The Van Krevelen (VK) diagram (Heald et al., 2010) provides valuable information on chemical evolution of OA as demonstrated by subsequent marine aerosols studies (Ovadnevaite et al. 2014; Willis et al. 2017; Dada et al. 2022). The VK plot of the PMF factors identified in this study superimposed with bulk OA O:C and H:C values is depicted in Figure 4. Overall, the bulk OA slope of -1.18 and $\overline{Osc}$ values spanning over -1.8 to 0.8 in the carbon oxidation state space indicates that higher levels of oxidation involving the generation of carboxylic acids, and the subsequent breakdown of the carbon backbone are prevalent over the measurement period which is consistent with MO-OOA functional groups (Heald *et al.*2010, Ng *et al.*, 2011). The O:C ratios for MO-OOA, PMOA and MSA-OA all fall within the range of 0.64–1.15 reported for diverse OOA factors from previous studies (Aiken et al., 2008; Jimenez et al., 2009). All PMF factors have H:C values lower than 2 which indicate that they all contain unsaturated carbons capable of reacting with O_3 (Ovadnevaite et al. 2011). This is evidenced by effective transfer entropy flow analysis (Behrendt et al., 2019) between Peat-OA, PMOA, MO-OOA, MSA-OA and O_3 values (Figure 43) which indicates that Peat-OA had the highest information transfer flow, making it the most susceptible to ozonolysis, closely followed by PMOA and, to a lesser extent, MSA-OA. Both Peat-OA (O:C=0.43, H:C=1.34) and PMOA (O:C=0.66, H:C=1.16) VK positions broadly fall in the area consistent with lignin-like compounds (H/C = 0.6–1.5, O/C = 0.1–0.6; Park et al. 2022) which have been largely associated with terrestrial origin OA (Jang et al., 2022) and found to be high in Arctic Ocean air masses as well (Choi et al., 2019) with authors reporting ~30% of the total assigned molecular formulae as marine lignin-like compounds. These lignin-like compounds are also know to oxidise and form Humic-like molecules, characterized by polar carbonyl (keto and carboxyl) functional groups alongside hydrophobic aliphatic chains (Cavalli, 2004) which broadly agrees with MO-OOA functional groups.

455 MSA-OA (O:C=0.66, H:C=1.9) is then also examined by colouring the VK scatter plot (Figure S8) with the
MSA-OA/SO$_4$ ratio, a proxy for biological marine sources contributions from DMS (Chen et al., 2021) with
values ranging from 0.001 (ubiquitous anthropogenic influences) to 0.354 (significant contribution from
biological marine sources) with an average value of 0.102 in line with pristine conditions (Huang et al., 2018).
Figure S8 shows that high MSA-to-sulphate ratio were consistent with VK region for C$_2$-C$_{12}$ saturated diacids
460 and inconsistent with C$_4$-C$_{12}$ carbohydrates and derivatives (trehalose, erythritol, arabitol, mannitol, sucrose,
galactose, glucose, fructose etc…) similarly to results reported for summertime Arctic (Willis et al., 2017).
However, as opposed to Artic aerosols, H:C ratios being higher, we report no association with VK areas for C$_4$
unsaturated diacids (e.g maleic and fumaric acid) nor with C$_{10}$ and C$_5$ keto-acids (levulinic and pinonic acid)
which are aqueous photochemistry tracers from isoprene and α-pinene oxidation (Kołodziejczyk et al., 2019;
465 Rapf et al., 2017). This is in line with the absence of other isoprene tracers; C$_4$H$_5^+$ (0.49%) at m/z 53.03 and
C$_5$H$_6$O$^+$ (0.18%) at m/z 82.04 (Hu et al., 2015; Robinson et al., 2011) and monoterpenes tracers (Boyd et al.,
2015), namely C$_5$H$_7^+$ at m/z 67.05 (0.15%) and (C$_7$H$_7^+$) at 91.05 (0.15%)-. This is also supported ~~with~~ by the lack
of covariance (Cov[X, Y] ≈ 0) between bulk CO$_2^+$, CO$^+$ and C$_2$H$_3$O$^+$ time series which also denotes the absence
of non-acid carbonyls (naCO) (Yazdani et al., 2022) which are known to be derived from isoprene and
470 monoterpenes (Russell et al. 2011). The reasons behind the absence of isoprene and monoterpenes influence on
OA in these findings are currently unclear although processes such as surface ocean consumption or unexplored
oxidations pathways could be a possibility (Benavent et al., 2022).
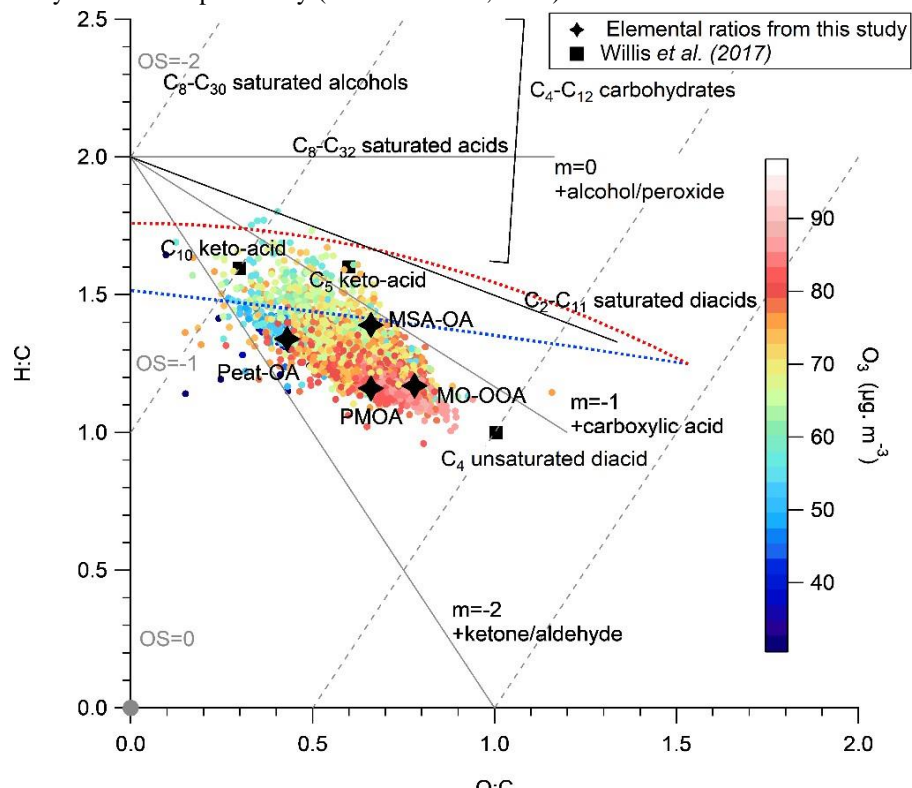
**Figure 4. Relationship between the ToF-AMS estimated hydrogen-to-carbon (H/C) and oxygen-to-carbon
(O/C) ratios of organic species [Canagaratna *et al*., 2015] coloured by O$_3$ mixing ratio, all observations above
475 ToF-AMS detection limits are shown for the entire period. Grey lines represent the ambient range of O/C
and H/C observed by Ng *et al*. [2011] while dashed line represent the average carbon oxidation state (OSc
≈ 2 × O : C − H : C) ~~(2011)~~ superimposed on the Van Krevelen diagram (Ng *et al*. 2011, Kroll *et al*., 2011).
Elemental composition of C$_8$–C$_{30}$ saturated alcohols, C$_8$–C$_{32}$ saturated acids, C$_2$ –C$_{11}$ saturated diacids, C$_4$**

unsaturated diacid (maleic and fumaric acid), C$_4$ – C$_{12}$ carbohydrates (e.g., trehalose, erythritol, arabitol, mannitol, sucrose, galactose, glucose, and fructose), and C$_5$ and C$_{10}$ ketoacids (levulinic and pinonic acid, respectively) are shown for reference (Willis *et al.*, 2017).

3.4 Air masses and source apportionment
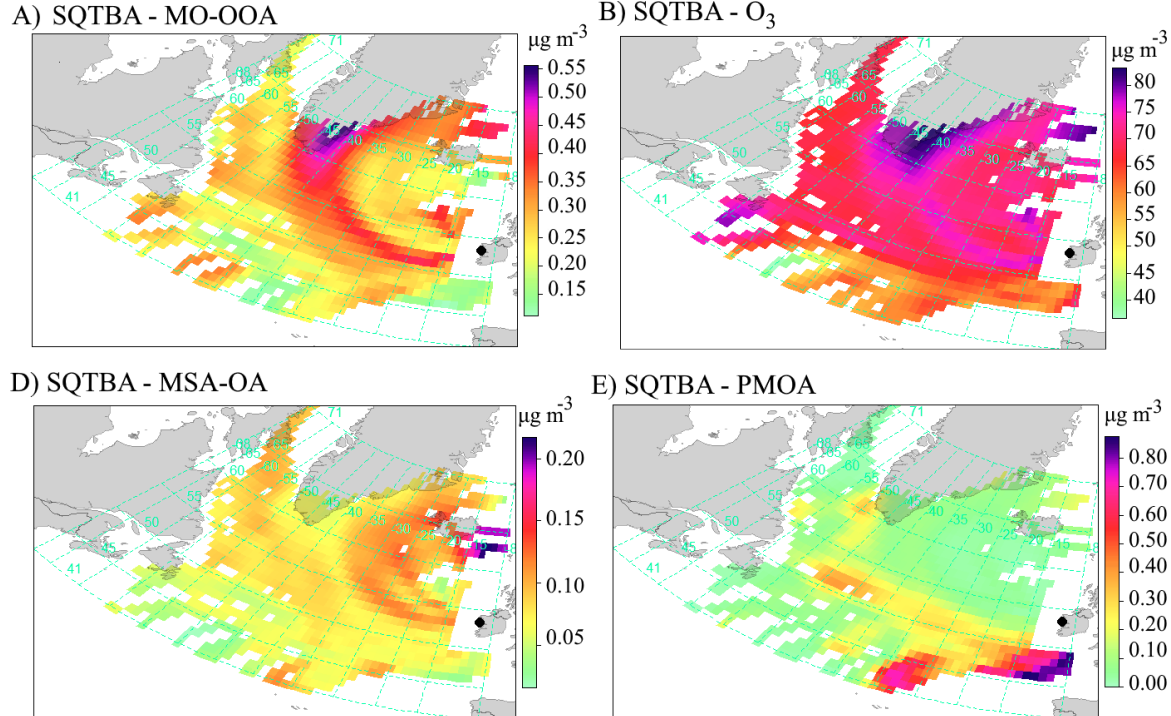
Figure 5. Simplified Quantitative Transport Bias Analysis (SQTBA) -Gaussian Air masses dispersion for PMF sources (PMOA, MO-OOA, MSA-OA) and O$_3$.

MO-OOA (Figure 5-A) strongest sources can be traced back northward along a cyclonic gradual crescent shape spreading from Greenland Seas South of Cape Farewell (See Figure S9 for Ocean areas toponomy). This culminates further with air masses origins spanning over the East Greenland Current (Denmark Strait), upwards to the Iceland Sea, south south of Jan Mayen. MO-OOA is otherwise ubiquitous and shows contributions over the Newfoundland, Labrador and Iceland basins as well as other areas. O$_3$ (Figure 5-B) shared similar origin as MO-OOA further confirming its role in MO-OOA formation. Overall, we observe aged polar air masses eventually flowing from Greenland to MHD. The sustained blockade and aging of air masses over Greenland is known and attributed to summertime high-pressure systems surrounding this region influenced by Arctic amplification (Pettersen et al., 2022; Preece et al., 2023) where the Irminger current Current also acts as a hotspot for turbulent eddies and heat transport which might contribute to aerosol nucleation (Semper et al., 2022). Here the presence of a blocking anticyclone transition (Figure S10) leading to reduced cloud cover and warm air advection might ultimately have contributed to an increase in aged SOA at the southern tip of Greenland possibly owing to its orography.
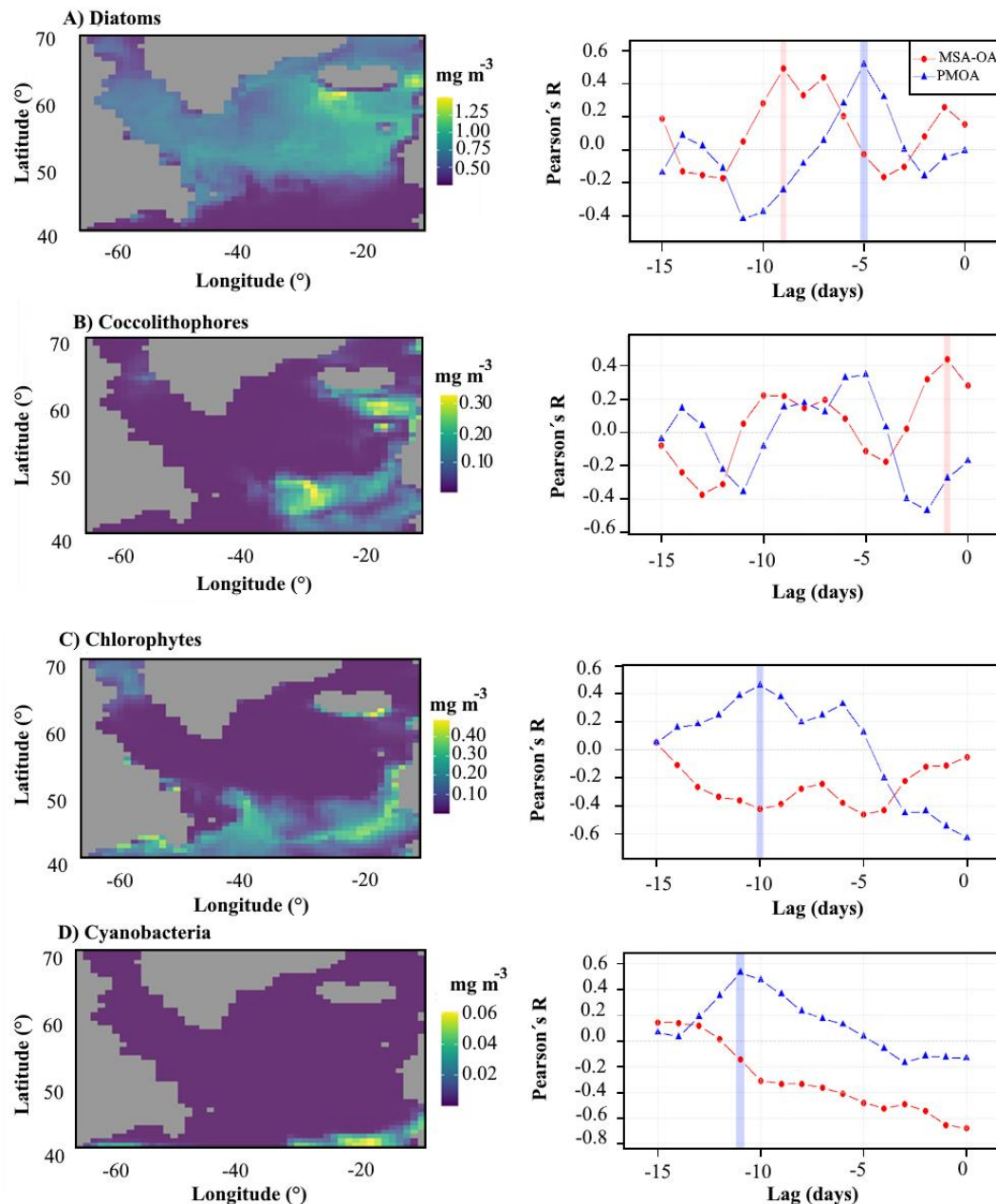
Figure 6. Time averaged maps (0.67 x 1.25 deg) over 2015-Aug, Region 59W, 37N, 34E, 82N of dominant phytoplankton groups from NOBM Model data (Rousseaux *et al*. 2017; Buchard *et al*. 2017) and corresponding lagged crossed correlations for MSA-OA (red) and PMOA (blue) against A) Diatoms B) Coccolithophores, C) Chlorophytes and D) Cyanobacteria ̶. The ̶ ̶blue and red shaded areas correspond to maximum significant crossed-correlations extracted from the autocorrelation function (ACF) ̶ 95% criteria.

MSA-OA (Figure 5-C) main sources include the Iceland basin and more specifically the Iceland-Faroe Ridge. This is consistent with literature highlighting the diversity of eukaryotic phytoplankton in the Icelandic marine environment with the haptophyte coccolithophore *Emiliania huxleyi* being dominant during summertime (Cerfonteyn et al., 2023) owing to nutrients transport by the North Atlantic Current acceleration (Oziel et al., 2020) and findings (O'Dowd *et al*. 2015: Mansour *et al*. 2023) indicating concomitant MSA concentrations uptick during summertime. MSA-OA also spans along the East Greenland Current (Denmark Strait) where wind-driven coastal upwelling (Håvik and Våge, 2018) might result in increased DMS emissions (Edtbauer et

al., 2020). Likewise, MSA-OA extend moderately over diverse regions such as the North-Western European Basin, the Newfoundland basin (where intense DMS fluxes have been reported; Bell *et al*. 2021) and the Labrador Sea.

PMOA (Figure 5-D) on the other hand strongly extends over the South of the Celtic Sea and West of the Bay of Biscay as well as West European basin waters and are otherwise diffused all over the North Atlantic Ocean with moderate intensity hotspots over the Newfoundland basin (Davis strait) possibly owing to an inflated subpolar gyre (Hátún et al., 2016).

Examination of NOBM model data (Figure 6) further reveals distinct MSA-OA and PMOA patterns. MSA-OA overlap with coccolithophores dominated ecoregions as well as diatoms ones. Similarly, diatoms also seem to contribute to PMOA sources, which is in line with recent results hypothesising that diatoms have a greater atmospheric significance than other eukaryotes due to their observed enrichment in PMOA (Alsante *et al*, 2021) whereas association with coccolithophores appears much weaker than for MSA-OA. Another distinction lies in PMOA overlapping with chlorophytes (*flagellates*, *Phaeocystis spp*) over the Western European basin. This geographic area hosts more than 512 chlorophyte species (Narayanaswamy et al., 2010) with recent reports of chlorophytes being one of the key contributors to marine productivity (Landwehr et al., 2021), further research is warranted to fully understand their role along other phytoplankton in this region during summertime. Likewise, cyanobacteria (combination of *Synechococcus*, *Prochlorococcus*, and nitrogen fixers such as *Trichodesmium*) might also contribute to PMOA more sparsely, especially at lower latitudes in the North Atlantic Ocean as previously reported (Baer et al., 2017).

Here, calculated lagged correlations (Figure 6) further pointed at MSA-OA being directly associated with coccolithophores (with a lag of -1 day) as well as diatoms (lag of -9 days), however no significant correlations were observed for either cyanobacteria or chlorophytes. As opposed to MSA-OA, the association between coccolithophores and PMOA doesn´t appear as meaningful (their autocorrelations are not statistically significant~~ly different from zero~~). PMOA on the other hand are also associated with diatoms (lag of -5 days) and show unique associations with chlorophytes (lag of -10 days) as well as cyanobacteria (lag of-11 days).

Overall, association between OA enriched sea spray time series and phytoplankton groups remains controversial owing to a wide range of governing mechanisms as highlighted by previous studies using chl-α as a proxy to calculate cross correlation time lags over the North Atlantic which were found to vary between 8 days (Rinaldi et al., 2013) and 24 days (O'Dowd et al., 2015) depending on the period and length of measurements.

Late summer measurements (Mansour et al., 2020) show partially comparable lags to this study with a reported oceanic biological activity affecting aerosol properties within the order of 10-20 days. This delay roughly spans over the full blooming to decaying phase transitions of an algal bloom (Lehahn et al., 2014) and is linked to the release of SSA-transferable organic matter in surface seawater by the interaction with marine viruses causing the demise of phytoplankton blooms (O'Dowd et al., 2015).

Here, by focusing on the lagged correlations between PMF factors and specific phytoplankton groups rather than bulk-OA and chl-α, this study´s findings indicate that PMOA is formed on such timescale from cyanobacteria and chlorophytes (lags of -11 and -10 days respectively) owing to atmospheric transport from the Western European basin whereas overwhelming diatoms influence results in a much shorter lag of -5 days. Additionally,

MSA-OA is rapidly produced from coccolithophores blooms in 1-2 days. This reflects stressed, senescent, grazed, or virus-infected phytoplankton releasing high quantities of DMSP which rapidly oxidises to form MSA-OA (Mansour et al., 2020).

Finally, the interpretation of diatoms´ role on either MSA-OA or PMOA remains ambiguous. The as the -5 days lag with PMOA could hint at lipase activity with concurring to self-aggregation and formation of free fatty acids during the bloom phase, during bloom potentially followed by a post-bloom phase (at a lag of -9 days with MSA-OA) with significantly different taxa. Alternatively, the -9 day lag with MSO-OA could have been or caused by simplyair advection from remote eco-regions further closer to thenear the Arctic which that have been reported to host rich MSA producing diatoms communities as opposed to more not present in the southerly latitudes (Becagli et al., 2016).

4. Conclusions

This study leverages high-resolution online aerosol mass spectrometry source apportionment to investigate the chemical composition and sources of submicron organic aerosols representing marine environment during a summertime period marked by phytoplankton blooms. The results emphasise balanced mass contributions from POA (PMOA and Peat-OA) and SOA (MO-OOA and MSA-OA), each category accounting for approximately 50% of the total submicron organic aerosol mass, with distinct chemical compositions reflective of their varied origins.

One of this study´s key finding is that summertime polar air masses undergo significant ozonolysis over the remote ocean which happens to be largely driven by the ageing of Greenland blocking blocked air masses aging and anticyclonic conditions. Transfer entropy is introduced here to explain the dynamics of ozonolysis in this context revealing significant information transfer to MO-OOA during unsaturated aliphatic chains (C=C double bonds) breakdown of PMOA as well as MSA-OA to a lesser extent. However, this transfer entropy approach additionally shows that MO-OOA is also being formed locally from Peat-OA oxidation, as such, further studies will aim at exactly delineating open ocean versus locally produced MO-OOA.

Another essential takeaway is that OA not only reflects atmospheric chemistry and meteorology but may also serve as an indicator of marine ecosystems (i.e. MSA-OA enzymes stress makers and PMOA phytoplankton extracellular metabolic processes markers). Air masses trajectory analysis also show reveal the source aerosols phytoplankton ecoregions. contributions with MSA-OA contributions are traced to the Iceland Basin and the Iceland-Faroe Ridge, with a rapid production burst (lag of 1-2 days) following coccolithophore blooms. Whereas relationship with diatoms show much longer lag (9 days) indicating fundamentally different oceanic biological processes. In contrast, PMOA is sourced from more diverse ecoregions (Southern Celtic Sea, West European Basin, and Newfoundland Basin), with additional chlorophytes and cyanobacteria influences from more southerly latitudes. All of this suggests that different phytoplankton taxa contributions to OA lead to specific m/z tracers and functional groups repartition (i.e. sulphides as coccolithophores tracers, aliphatics as tracers for diatoms) though further investigation is needed to explore the biological processes and ecoregions specificities influencing this relationship. Overall, this study demonstrates the complex aerosol chemistry and diverse geographic origins influencing POA and SOA formation in the Northeast Atlantic marine environment.

Our findings emphasise the need for further long-term investigation to fully account for the various precursors and pathways contributing to OA, given their significant impacts on aerosol-climate interactions.

Competing interests. The authors declare that they have no conflict of interest.

Acknowledgments. This work was supported by the EPA-Ireland and Department of the Environment, Climate and Communications and University of Galway College of Science and Engineering Postgraduate Fellowship n°127407. C. Lin acknowledges the support from the International Partnership Program of the Chinese Academy of Sciences (Grant No. 175GJHZ2022039FN). The authors would also like to acknowledge the support from the SFI FFP award (22/FFP-A/10611). Finally, we would also like to extend our gratitude to Seraphine Hauser for looking into geopotential height anomalies and producing figure S10.

Data availability. Data available upon request. *The NASA Ocean Biogeochemical Model output data was obtained with the Giovanni online data system, developed and maintained by the NASA GES DISC. The ERA5 boundary layer data are available at the Copernicus Climate Data Store portal (Hersbach et al., 2020).*

References

Aguilera, A., Distéfano, A., Jauzein, C., Correa-Aragunde, N., Martinez, D., Martin, M. V., and Sueldo, D. J.: Do photosynthetic cells communicate with each other during cell death? From cyanobacteria to vascular plants, Journal of Experimental Botany, 73, 7219–7242, https://doi.org/10.1093/jxb/erac363, 2022.

Aiken, A. C., DeCarlo, P. F., Kroll, J. H., Worsnop, D. R., Huffman, J. A., Docherty, K. S., Ulbrich, I. M., Mohr, C., Kimmel, J. R., Sueper, D., Sun, Y., Zhang, Q., Trimborn, A., Northway, M., Ziemann, P. J., Canagaratna, M. R., Onasch, T. B., Alfarra, M. R., Prevot, A. S. H., Dommen, J., Duplissy, J., Metzger, A., Baltensperger, U., and Jimenez, J. L.: O/C and OM/OC Ratios of Primary, Secondary, and Ambient Organic Aerosols with High-Resolution Time-of-Flight Aerosol Mass Spectrometry, Environ. Sci. Technol., 42, 4478–4485, https://doi.org/10.1021/es703009q, 2008.

Alsante, A. N., Thornton, D. C. O., and Brooks, S. D.: Ocean Aerobiology, Front. Microbiol., 12, 764178, https://doi.org/10.3389/fmicb.2021.764178, 2021.

Asch, R. G., Stock, C. A., and Sarmiento, J. L.: Climate change impacts on mismatches between phytoplankton blooms and fish spawning phenology, Global Change Biology, 25, 2544–2559, https://doi.org/10.1111/gcb.14650, 2019.

Baer, S. E., Lomas, M. W., Terpis, K. X., Mouginot, C., and Martiny, A. C.: Stoichiometry of *Prochlorococcus, Synechococcus* , and small eukaryotic populations in the western North Atlantic Ocean, Environmental Microbiology, 19, 1568–1583, https://doi.org/10.1111/1462-2920.13672, 2017.

Bahadur, R., Uplinger, T., Russell, L. M., Sive, B. C., Cliff, S. S., Millet, D. B., Goldstein, A., and Bates, T. S.: Phenol Groups in Northeastern U.S. Submicrometer Aerosol Particles Produced from Seawater Sources, Environ. Sci. Technol., 44, 2542–2548, https://doi.org/10.1021/es9032277, 2010.

Ban, Z., Hu, X., and Li, J.: Tipping points of marine phytoplankton to multiple environmental stressors, Nat. Clim. Chang., 12, 1045–1051, https://doi.org/10.1038/s41558-022-01489-0, 2022.

Bates, T. S., Quinn, P. K., Frossard, A. A., Russell, L. M., Hakala, J., Petäjä, T., Kulmala, M., Covert, D. S., Cappa, C. D., Li, S.-M., Hayden, K. L., Nuaaman, I., McLaren, R., Massoli, P., Canagaratna, M. R., Onasch, T. B., Sueper, D., Worsnop, D. R., and Keene, W. C.: Measurements of ocean derived aerosol off the coast of California: MEASUREMENTS OF OCEAN DERIVED AEROSOL, J. Geophys. Res., 117, n/a-n/a, https://doi.org/10.1029/2012JD017588, 2012.

Becagli, S., Lazzara, L., Marchese, C., Dayan, U., Ascanius, S. E., Cacciani, M., Caiazzo, L., Di Biagio, C., Di Iorio, T., Di Sarra, A., Eriksen, P., Fani, F., Giardi, F., Meloni, D., Muscari, G., Pace, G., Severi, M., Traversi, R., and Udisti, R.: Relationships linking primary production, sea ice melting, and biogenic aerosol in the Arctic, Atmospheric Environment, 136, 1–15, https://doi.org/10.1016/j.atmosenv.2016.04.002, 2016.

Becagli, S., Amore, A., Caiazzo, L., Iorio, T. D., Sarra, A. D., Lazzara, L., Marchese, C., Meloni, D., Mori, G., Muscari, G., Nuccio, C., Pace, G., Severi, M., and Traversi, R.: Biogenic Aerosol in the Artic from Eight Years of MSA Data from Ny Ålesund (Svalbard Islands) and Thule (Greenland), Atmosphere, 10, 349, https://doi.org/10.3390/atmos10070349, 2019.

Bedford, J., Ostle, C., Johns, D. G., Atkinson, A., Best, M., Bresnan, E., Machairopoulou, M., Graves, C. A., Devlin, M., Milligan, A., Pitois, S., Mellor, A., Tett, P., and McQuatters‐Gollop, A.: Lifeform indicators reveal large‐scale shifts in plankton across the North‐West European shelf, Global Change Biology, 26, 3482–3497, https://doi.org/10.1111/gcb.15066, 2020.

Behrendt, S., Dimpfl, T., Peter, F. J., and Zimmermann, D. J.: RTransferEntropy — Quantifying information flow between different time series using effective transfer entropy, SoftwareX, 10, 100265, https://doi.org/10.1016/j.softx.2019.100265, 2019.

Behrenfeld, M. J., Moore, R. H., Hostetler, C. A., Graff, J., Gaube, P., Russell, L. M., Chen, G., Doney, S. C., Giovannoni, S., Liu, H., Proctor, C., Bolaños, L. M., Baetge, N., Davie-Martin, C., Westberry, T. K., Bates, T. S., Bell, T. G., Bidle, K. D., Boss, E. S., Brooks, S. D., Cairns, B., Carlson, C., Halsey, K., Harvey, E. L., Hu, C., Karp-Boss, L., Kleb, M., Menden-Deuer, S., Morison, F., Quinn, P. K., Scarino, A. J., Anderson, B., Chowdhary, J., Crosbie, E., Ferrare, R., Hair, J. W., Hu, Y., Janz, S., Redemann, J., Saltzman, E., Shook, M., Siegel, D. A., Wisthaler, A., Martin, M. Y., and Ziemba, L.: The North Atlantic Aerosol and Marine Ecosystem Study (NAAMES): Science Motive and Mission Overview, Front. Mar. Sci., 6, 122, https://doi.org/10.3389/fmars.2019.00122, 2019.

Bell, T. G., Porter, J. G., Wang, W.-L., Lawler, M. J., Boss, E., Behrenfeld, M. J., and Saltzman, E. S.: Predictability of Seawater DMS During the North Atlantic Aerosol and Marine Ecosystem Study (NAAMES), Front. Mar. Sci., 7, 596763, https://doi.org/10.3389/fmars.2020.596763, 2021.

Benavent, N., Mahajan, A. S., Li, Q., Cuevas, C. A., Schmale, J., Angot, H., Jokinen, T., Quéléver, L. L. J., Blechschmidt, A.-M., Zilker, B., Richter, A., Serna, J. A., Garcia-Nieto, D., Fernandez, R. P., Skov, H., Dumitrascu, A., Simões Pereira, P., Abrahamsson, K., Bucci, S., Duetsch, M., Stohl, A., Beck, I., Laurila, T., Blomquist, B., Howard, D., Archer, S. D., Bariteau, L., Helmig, D., Hueber, J., Jacobi, H.-W., Posman, K., Dada, L., Daellenbach, K. R., and Saiz-Lopez, A.: Substantial contribution of iodine to Arctic ozone destruction, Nat. Geosci., https://doi.org/10.1038/s41561-022-01018-w, 2022.

Bian, H., Froyd, K., Murphy, D. M., Dibb, J., Darmenov, A., Chin, M., Colarco, P. R., Da Silva, A., Kucsera, T. L., Schill, G., Yu, H., Bui, P., Dollner, M., Weinzierl, B., and Smirnov, A.: Observationally constrained analysis of sea salt aerosol in the marine atmosphere, Atmos. Chem. Phys., 19, 10773–10785, https://doi.org/10.5194/acp-19-10773-2019, 2019.

Bigg, E. K. and Leck, C.: The composition of fragments of bubbles bursting at the ocean surface, J. Geophys. Res., 113, D11209, https://doi.org/10.1029/2007JD009078, 2008.

Bork, N., Elm, J., Olenius, T., and Vehkamäki, H.: Methane sulfonic acid-enhanced formation of molecular clusters of sulfuric acid and dimethyl amine, Atmos. Chem. Phys., 14, 12023–12030, https://doi.org/10.5194/acp-14-12023-2014, 2014.

Boyd, C. M., Sanchez, J., Xu, L., Eugene, A. J., Nah, T., Tuet, W. Y., Guzman, M. I., and Ng, N. L.: Secondary organic aerosol formation from the β-pinene+NO$_3$ system: effect of humidity and peroxy radical fate, Atmos. Chem. Phys., 15, 7497–7522, https://doi.org/10.5194/acp-15-7497-2015, 2015.

Brüggemann, M., Hayeck, N., and George, C.: Interfacial photochemistry at the ocean surface is a global source of organic vapors and aerosols, Nat Commun, 9, 2101, https://doi.org/10.1038/s41467-018-04528-7, 2018.

Canagaratna, M. R., Jayne, J. T., Jimenez, J. L., Allan, J. D., Alfarra, M. R., Zhang, Q., Onasch, T. B., Drewnick, F., Coe, H., Middlebrook, A., Delia, A., Williams, L. R., Trimborn, A. M., Northway, M. J., DeCarlo,

P. F., Kolb, C. E., Davidovits, P., and Worsnop, D. R.: Chemical and microphysical characterization of ambient aerosols with the aerodyne aerosol mass spectrometer, Mass Spectrom. Rev., 26, 185–222, https://doi.org/10.1002/mas.20115, 2007.

685   Canagaratna, M. R., Jimenez, J. L., Kroll, J. H., Chen, Q., Kessler, S. H., Massoli, P., Hildebrandt Ruiz, L., Fortner, E., Williams, L. R., Wilson, K. R., Surratt, J. D., Donahue, N. M., Jayne, J. T., and Worsnop, D. R.: Elemental ratio measurements of organic compounds using aerosol mass spectrometry: characterization, improved calibration, and implications, Atmos. Chem. Phys., 15, 253–272, https://doi.org/10.5194/acp-15-253-2015, 2015.

690   Canonaco, F., Crippa, M., Slowik, J. G., Baltensperger, U., and Prévôt, A. S. H.: SoFi, an IGOR-based interface for the efficient use of the generalized multilinear engine (ME-2) for the source apportionment: ME-2 application to aerosol mass spectrometer data, Atmos. Meas. Tech., 6, 3649–3661, https://doi.org/10.5194/amt-6-3649-2013, 2013.

695   Canonaco, F., Tobler, A., Chen, G., Sosedova, Y., Slowik, J. G., Bozzetti, C., Daellenbach, K. R., El Haddad, I., Crippa, M., Huang, R.-J., Furger, M., Baltensperger, U., and Prévôt, A. S. H.: A new method for long-term source apportionment with time-dependent factor profiles and uncertainty assessment using SoFi Pro: application to 1 year of organic aerosol data, Atmos. Meas. Tech., 14, 923–943, https://doi.org/10.5194/amt-14-923-2021, 2021.

700   Carslaw, K. S., Gordon, H., Hamilton, D. S., Johnson, J. S., Regayre, L. A., Yoshioka, M., and Pringle, K. J.: Aerosols in the Pre-industrial Atmosphere, Curr Clim Change Rep, 3, 1–15, https://doi.org/10.1007/s40641-017-0061-2, 2017.

Cavalli, F.: Advances in characterization of size-resolved organic matter in marine aerosol over the North Atlantic, J. Geophys. Res., 109, D24215, https://doi.org/10.1029/2004JD005137, 2004.

705   Ceburnis, D., Garbaras, A., Szidat, S., Rinaldi, M., Fahrni, S., Perron, N., Wacker, L., Leinert, S., Remeikis, V., Facchini, M. C., Prevot, A. S. H., Jennings, S. G., Ramonet, M., and O'Dowd, C. D.: Quantification of the carbonaceous matter origin in submicron marine aerosol by ^{13}C and ^{14}C isotope analysis, Atmos. Chem. Phys., 11, 8593–8606, https://doi.org/10.5194/acp-11-8593-2011, 2011.

710   Cerfonteyn, M., Groben, R., Vaulot, D., Guðmundsson, K., Vannier, P., Pérez-Hernández, M. D., and Marteinsson, V. Þ.: The distribution and diversity of eukaryotic phytoplankton in the Icelandic marine environment, Sci Rep, 13, 8519, https://doi.org/10.1038/s41598-023-35537-2, 2023.

Chen, D., Shen, Y., Wang, J., Gao, Y., Gao, H., and Yao, X.: Mapping gaseous dimethylamine, trimethylamine, ammonia, and their particulate counterparts in marine atmospheres of China's marginal seas – Part 1: Differentiating marine emission from continental transport, Atmos. Chem. Phys., 21, 16413–16425, https://doi.org/10.5194/acp-21-16413-2021, 2021.

715   Chen, H., Varner, M. E., Gerber, R. B., and Finlayson-Pitts, B. J.: Reactions of Methanesulfonic Acid with Amines and Ammonia as a Source of New Particles in Air, J. Phys. Chem. B, 120, 1526–1536, https://doi.org/10.1021/acs.jpcb.5b07433, 2016.

Choi, J. H., Jang, E., Yoon, Y. J., Park, J. Y., Kim, T. -W., Becagli, S., Caiazzo, L., Cappelletti, D., Krejci, R., Eleftheriadis, K., Park, K. -T., and Jang, K. S.: Influence of Biogenic Organics on the Chemical Composition of 720   Arctic Aerosols, Global Biogeochemical Cycles, 33, 1238–1250, https://doi.org/10.1029/2019GB006226, 2019.

Cochran, R. E., Laskina, O., Trueblood, J. V., Estillore, A. D., Morris, H. S., Jayarathne, T., Sultana, C. M., Lee, C., Lin, P., Laskin, J., Laskin, A., Dowling, J. A., Qin, Z., Cappa, C. D., Bertram, T. H., Tivanski, A. V., Stone, E. A., Prather, K. A., and Grassian, V. H.: Molecular Diversity of Sea Spray Aerosol Particles: Impact of Ocean Biology on Particle Composition and Hygroscopicity, Chem, 2, 655–667, 725   https://doi.org/10.1016/j.chempr.2017.03.007, 2017.

Crippa, M., El Haddad, I., Slowik, J. G., DeCarlo, P. F., Mohr, C., Heringa, M. F., Chirico, R., Marchand, N., Sciare, J., Baltensperger, U., and Prévôt, A. S. H.: Identification of marine and continental aerosol sources in

Paris using high resolution aerosol mass spectrometry: AEROSOL SOURCES IN PARIS USING HR-TOF-MS, J. Geophys. Res. Atmos., 118, 1950–1963, https://doi.org/10.1002/jgrd.50151, 2013.

730 Croft, B., Martin, R. V., Moore, R. H., Ziemba, L. D., Crosbie, E. C., Liu, H., Russell, L. M., Saliba, G., Wisthaler, A., Müller, M., Schiller, A., Galí, M., Chang, R. Y.-W., McDuffie, E. E., Bilsback, K. R., and Pierce, J. R.: Factors controlling marine aerosol size distributions and their climate effects over the northwest Atlantic Ocean region, Atmos. Chem. Phys., 21, 1889–1916, https://doi.org/10.5194/acp-21-1889-2021, 2021.

Cubison, M. J., Ortega, A. M., Hayes, P. L., Farmer, D. K., Day, D., Lechner, M. J., Brune, W. H., Apel, E., 735 Diskin, G. S., Fisher, J. A., Fuelberg, H. E., Hecobian, A., Knapp, D. J., Mikoviny, T., Riemer, D., Sachse, G. W., Sessions, W., Weber, R. J., Weinheimer, A. J., Wisthaler, A., and Jimenez, J. L.: Effects of aging on organic aerosol from open biomass burning smoke in aircraft and laboratory studies, Atmos. Chem. Phys., 11, 12049–12064, https://doi.org/10.5194/acp-11-12049-2011, 2011.

Cui, S., Huang, D. D., Wu, Y., Wang, J., Shen, F., Xian, J., Zhang, Y., Wang, H., Huang, C., Liao, H., and Ge, 740 X.: Chemical properties, sources and size-resolved hygroscopicity of submicron black-carbon-containing aerosols in urban Shanghai, Atmos. Chem. Phys., 22, 8073–8096, https://doi.org/10.5194/acp-22-8073-2022, 2022.

Dada, L., Angot, H., Beck, I., Baccarini, A., Quéléver, L. L. J., Boyer, M., Laurila, T., Brasseur, Z., Jozef, G., De Boer, G., Shupe, M. D., Henning, S., Bucci, S., Dütsch, M., Stohl, A., Petäjä, T., Daellenbach, K. R., Jokinen, 745 T., and Schmale, J.: A central arctic extreme aerosol event triggered by a warm air-mass intrusion, Nat Commun, 13, 5290, https://doi.org/10.1038/s41467-022-32872-2, 2022.

DeCarlo, P. F., Kimmel, J. R., Trimborn, A., Northway, M. J., Jayne, J. T., Aiken, A. C., Gonin, M., Fuhrer, K., Horvath, T., Docherty, K. S., Worsnop, D. R., and Jimenez, J. L.: Field-Deployable, High-Resolution, Time-of-Flight Aerosol Mass Spectrometer, Anal. Chem., 78, 8281–8289, https://doi.org/10.1021/ac061249n, 2006.

750 Decesari, S., Mircea, M., Cavalli, F., Fuzzi, S., Moretti, F., Tagliavini, E., and Facchini, M. C.: Source Attribution of Water-Soluble Organic Aerosol by Nuclear Magnetic Resonance Spectroscopy, Environ. Sci. Technol., 41, 2479–2484, https://doi.org/10.1021/es061711l, 2007.

Derwent, R. G., Simmonds, P. G., and Collins, W. J.: Ozone and carbon monoxide measurements at a remote maritime location, mace head, Ireland, from 1990 to 1992, Atmospheric Environment, 28, 2623–2637, 755 https://doi.org/10.1016/1352-2310(94)90436-7, 1994.

Derwent, R. G., Manning, A. J., Simmonds, P. G., Spain, T. G., and O'Doherty, S.: Long-term trends in ozone in baseline and European regionally-polluted air at Mace Head, Ireland over a 30-year period, Atmospheric Environment, 179, 279–287, https://doi.org/10.1016/j.atmosenv.2018.02.024, 2018.

Dominutti, P. A., Chevassus, E., Baray, J.-L., Jaffrezo, J.-L., Borbon, A., Colomb, A., Deguillaume, L., El 760 Gdachi, S., Houdier, S., Leriche, M., Metzger, J.-M., Rocco, M., Tulet, P., Sellegri, K., and Freney, E.: Evaluation of the Sources, Precursors, and Processing of Aerosols at a High-Altitude Tropical Site, ACS Earth Space Chem., 6, 2412–2431, https://doi.org/10.1021/acsearthspacechem.2c00149, 2022.

Drewnick, F., Hings, S. S., Alfarra, M. R., Prevot, A. S. H., and Borrmann, S.: Aerosol quantification with the Aerodyne Aerosol Mass Spectrometer: detection limits and ionizer background effects, Atmos. Meas. Tech., 2, 765 33–46, https://doi.org/10.5194/amt-2-33-2009, 2009.

Duplissy, J., DeCarlo, P. F., Dommen, J., Alfarra, M. R., Metzger, A., Barmpadimos, I., Prevot, A. S. H., Weingartner, E., Tritscher, T., Gysel, M., Aiken, A. C., Jimenez, J. L., Canagaratna, M. R., Worsnop, D. R., Collins, D. R., Tomlinson, J., and Baltensperger, U.: Relating hygroscopicity and composition of organic aerosol particulate matter, Atmos. Chem. Phys., 11, 1155–1165, https://doi.org/10.5194/acp-11-1155-2011, 2011.

770 Edtbauer, A., Stönner, C., Pfannerstill, E. Y., Berasategui, M., Walter, D., Crowley, J. N., Lelieveld, J., and Williams, J.: A new marine biogenic emission: methane sulfonamide (MSAM), dimethyl sulfide (DMS), and dimethyl sulfone (DMSO$_2$) measured in air over the Arabian Sea, Atmos. Chem. Phys., 20, 6081–6094, https://doi.org/10.5194/acp-20-6081-2020, 2020.

775 Etminan, M., Myhre, G., Highwood, E. J., and Shine, K. P.: Radiative forcing of carbon dioxide, methane, and nitrous oxide: A significant revision of the methane radiative forcing, Geophys. Res. Lett., 43, https://doi.org/10.1002/2016GL071930, 2016.

Facchini, M. C., Rinaldi, M., Decesari, S., Carbone, C., Finessi, E., Mircea, M., Fuzzi, S., Ceburnis, D., Flanagan, R., Nilsson, E. D., de Leeuw, G., Martino, M., Woeltjen, J., and O'Dowd, C. D.: Primary submicron marine aerosol dominated by insoluble organic colloids and aggregates, Geophys. Res. Lett., 35, L17814, 780 https://doi.org/10.1029/2008GL034210, 2008.

Faiola, C. L., Wen, M., and VanReken, T. M.: Chemical characterization of biogenic secondary organic aerosol generated from plant emissions under baseline and stressed conditions: inter- and intra-species variability for six coniferous species, Atmos. Chem. Phys., 15, 3629–3646, https://doi.org/10.5194/acp-15-3629-2015, 2015.

Flerus, R., Lechtenfeld, O. J., Koch, B. P., McCallister, S. L., Schmitt-Kopplin, P., Benner, R., Kaiser, K., and 785 Kattner, G.: A molecular perspective on the ageing of marine dissolved organic matter, Biogeosciences, 9, 1935–1955, https://doi.org/10.5194/bg-9-1935-2012, 2012.

Florou, K., Liangou, A., Kaltsonoudis, C., Louvaris, E., Tasoglou, A., Patoulias, D., Kouvarakis, G., Kalivitis, N., Kourtchev, I., Kalberer, M., Tsagkaraki, M., Mihalopoulos, N., and Pandis, S. N.: Chemical characterization and sources of background aerosols in the eastern Mediterranean, Atmospheric Environment, 324, 120423, 790 https://doi.org/10.1016/j.atmosenv.2024.120423, 2024.

Fossum, K. N., Ovadnevaite, J., Ceburnis, D., Dall'Osto, M., Marullo, S., Bellacicco, M., Simó, R., Liu, D., Flynn, M., Zuend, A., and O'Dowd, C.: Summertime Primary and Secondary Contributions to Southern Ocean Cloud Condensation Nuclei, Sci Rep, 8, 13844, https://doi.org/10.1038/s41598-018-32047-4, 2018.

Fröhlich, R., Crenn, V., Setyan, A., Belis, C. A., Canonaco, F., Favez, O., Riffault, V., Slowik, J. G., Aas, W., 795 Aijälä, M., Alastuey, A., Artiñano, B., Bonnaire, N., Bozzetti, C., Bressi, M., Carbone, C., Coz, E., Croteau, P. L., Cubison, M. J., Esser-Gietl, J. K., Green, D. C., Gros, V., Heikkinen, L., Herrmann, H., Jayne, J. T., Lunder, C. R., Minguillón, M. C., Močnik, G., O'Dowd, C. D., Ovadnevaite, J., Petralia, E., Poulain, L., Priestman, M., Ripoll, A., Sarda-Estève, R., Wiedensohler, A., Baltensperger, U., Sciare, J., and Prévôt, A. S. H.: ACTRIS ACSM intercomparison – Part 2: Intercomparison of ME-2 organic source apportionment results from 15 800 individual, co-located aerosol mass spectrometers, Atmos. Meas. Tech., 8, 2555–2576, https://doi.org/10.5194/amt-8-2555-2015, 2015.

Giordano, M. R., Kalnajs, L. E., Avery, A., Goetz, J. D., Davis, S. M., and DeCarlo, P. F.: A missing source of aerosols in Antarctica – beyond long-range transport, phytoplankton, and photochemistry, Aerosols/Field Measurements/Troposphere/Chemistry (chemical composition and reactions), https://doi.org/10.5194/acp-2016-805 606, 2016.

Glicker, H. S., Lawler, M. J., Chee, S., Resch, J., Garofalo, L. A., Mayer, K. J., Prather, K. A., Farmer, D. K., and Smith, J. N.: Chemical Composition of an Ultrafine Sea Spray Aerosol during the Sea Spray Chemistry and Particle Evolution Experiment, ACS Earth Space Chem., 6, 1914–1923, https://doi.org/10.1021/acsearthspacechem.2c00127, 2022.

810 Goldstein, A. H. and Galbally, I. E.: Known and Unexplored Organic Constituents in the Earth's Atmosphere, Environ. Sci. Technol., 41, 1514–1521, https://doi.org/10.1021/es072476p, 2007.

Grigas, T., Ovadnevaite, J., Ceburnis, D., Moran, E., McGovern, F. M., Jennings, S. G., and O'Dowd, C.: Sophisticated Clean Air Strategies Required to Mitigate Against Particulate Organic Pollution, Sci Rep, 7, 44737, https://doi.org/10.1038/srep44737, 2017.

815 Gryspeerdt, E., Povey, A. C., Grainger, R. G., Hasekamp, O., Hsu, N. C., Mulcahy, J. P., Sayer, A. M., and Sorooshian, A.: Uncertainty in aerosol–cloud radiative forcing is driven by clean conditions, Atmos. Chem. Phys., 23, 4115–4122, https://doi.org/10.5194/acp-23-4115-2023, 2023.

Guo, J., Zhang, J., Yang, K., Liao, H., Zhang, S., Huang, K., Lv, Y., Shao, J., Yu, T., Tong, B., Li, J., Su, T., Yim, S. H. L., Stoffelen, A., Zhai, P., and Xu, X.: Investigation of near-global daytime boundary layer height 820 using high-resolution radiosondes: first results and comparison with ERA5, MERRA-2, JRA-55, and NCEP-2 reanalyses, Atmos. Chem. Phys., 21, 17079–17097, https://doi.org/10.5194/acp-21-17079-2021, 2021.

Hallquist, M., Wenger, J. C., Baltensperger, U., Rudich, Y., Simpson, D., Claeys, M., Dommen, J., Donahue, N. M., George, C., Goldstein, A. H., Hamilton, J. F., Herrmann, H., Hoffmann, T., Iinuma, Y., Jang, M., Jenkin, M. E., Jimenez, J. L., Kiendler-Scharr, A., Maenhaut, W., McFiggans, G., Mentel, Th. F., Monod, A., Prévôt, A. S. H., Seinfeld, J. H., Surratt, J. D., Szmigielski, R., and Wildt, J.: The formation, properties and impact of secondary organic aerosol: current and emerging issues, Atmos. Chem. Phys., 9, 5155–5236, https://doi.org/10.5194/acp-9-5155-2009, 2009.

Hátún, H., Lohmann, K., Matei, D., Jungclaus, J. H., Pacariz, S., Bersch, M., Gislason, A., Ólafsson, J., and Reid, P. C.: An inflated subpolar gyre blows life toward the northeastern Atlantic, Progress in Oceanography, 147, 49–66, https://doi.org/10.1016/j.pocean.2016.07.009, 2016.

Håvik, L. and Våge, K.: Wind-Driven Coastal Upwelling and Downwelling in the Shelfbreak East Greenland Current, JGR Oceans, 123, 6106–6115, https://doi.org/10.1029/2018JC014273, 2018.

Heald, C. L., Kroll, J. H., Jimenez, J. L., Docherty, K. S., DeCarlo, P. F., Aiken, A. C., Chen, Q., Martin, S. T., Farmer, D. K., and Artaxo, P.: A simplified description of the evolution of organic aerosol composition in the atmosphere: VAN KREVELEN DIAGRAM OF ORGANIC AEROSOL, Geophys. Res. Lett., 37, https://doi.org/10.1029/2010GL042737, 2010.

Hersbach, H., Bell, B., Berrisford, P., Hirahara, S., Horányi, A., Muñoz-Sabater, J., Nicolas, J., Peubey, C., Radu, R., Schepers, D., Simmons, A., Soci, C., Abdalla, S., Abellan, X., Balsamo, G., Bechtold, P., Biavati, G., Bidlot, J., Bonavita, M., Chiara, G., Dahlgren, P., Dee, D., Diamantakis, M., Dragani, R., Flemming, J., Forbes, R., Fuentes, M., Geer, A., Haimberger, L., Healy, S., Hogan, R. J., Hólm, E., Janisková, M., Keeley, S., Laloyaux, P., Lopez, P., Lupu, C., Radnoti, G., Rosnay, P., Rozum, I., Vamborg, F., Villaume, S., and Thépaut, J.: The ERA5 global reanalysis, Q.J.R. Meteorol. Soc., 146, 1999–2049, https://doi.org/10.1002/qj.3803, 2020.

Hodshire, A. L., Campuzano-Jost, P., Kodros, J. K., Croft, B., Nault, B. A., Schroder, J. C., Jimenez, J. L., and Pierce, J. R.: The potential role of methanesulfonic acid (MSA) in aerosol formation and growth and the associated radiative forcings, Atmos. Chem. Phys., 19, 3137–3160, https://doi.org/10.5194/acp-19-3137-2019, 2019.

Holland, M. M., Louchart, A., Artigas, L. F., Ostle, C., Atkinson, A., Rombouts, I., Graves, C. A., Devlin, M., Heyden, B., Machairopoulou, M., Bresnan, E., Schilder, J., Jakobsen, H. H., Lloyd-Hartley, H., Tett, P., Best, M., Goberville, E., and McQuatters-Gollop, A.: Major declines in NE Atlantic plankton contrast with more stable populations in the rapidly warming North Sea, Science of The Total Environment, 898, 165505, https://doi.org/10.1016/j.scitotenv.2023.165505, 2023.

Hu, W. W., Campuzano-Jost, P., Palm, B. B., Day, D. A., Ortega, A. M., Hayes, P. L., Krechmer, J. E., Chen, Q., Kuwata, M., Liu, Y. J., de Sá, S. S., McKinney, K., Martin, S. T., Hu, M., Budisulistiorini, S. H., Riva, M., Surratt, J. D., St. Clair, J. M., Isaacman-Van Wertz, G., Yee, L. D., Goldstein, A. H., Carbone, S., Brito, J., Artaxo, P., de Gouw, J. A., Koss, A., Wisthaler, A., Mikoviny, T., Karl, T., Kaser, L., Jud, W., Hansel, A., Docherty, K. S., Alexander, M. L., Robinson, N. H., Coe, H., Allan, J. D., Canagaratna, M. R., Paulot, F., and Jimenez, J. L.: Characterization of a real-time tracer for isoprene epoxydiols-derived secondary organic aerosol (IEPOX-SOA) from aerosol mass spectrometer measurements, Atmos. Chem. Phys., 15, 11807–11833, https://doi.org/10.5194/acp-15-11807-2015, 2015.

Huang, S., Wu, Z., Poulain, L., van Pinxteren, M., Merkel, M., Assmann, D., Herrmann, H., and Wiedensohler, A.: Source apportionment of the organic aerosol over the Atlantic Ocean from 53° N to 53° S: significant contributions from marine emissions and long-range transport, Atmos. Chem. Phys., 18, 18043–18062, https://doi.org/10.5194/acp-18-18043-2018, 2018.

Huffman, J. A., Jayne, J. T., Drewnick, F., Aiken, A. C., Onasch, T., Worsnop, D. R., and Jimenez, J. L.: Design, Modeling, Optimization, and Experimental Tests of a Particle Beam Width Probe for the Aerodyne Aerosol Mass Spectrometer, Aerosol Science and Technology, 39, 1143–1163, https://doi.org/10.1080/02786820500423782, 2005.

Jang, J., Park, J., Park, J., Yoon, Y. J., Dall'Osto, M. s., Park, K.-T., Jang, E., Lee, J., Cho, K. H., and Lee, B. Y.: Ocean-Atmosphere Interactions: Different Organic Components Across Pacific and Southern Oceans, SSRN Journal, https://doi.org/10.2139/ssrn.4290253, 2022.

Jimenez, J. L., Canagaratna, M. R., Donahue, N. M., Prevot, A. S. H., Zhang, Q., Kroll, J. H., DeCarlo, P. F., Allan, J. D., Coe, H., Ng, N. L., Aiken, A. C., Docherty, K. S., Ulbrich, I. M., Grieshop, A. P., Robinson, A. L., Duplissy, J., Smith, J. D., Wilson, K. R., Lanz, V. A., Hueglin, C., Sun, Y. L., Tian, J., Laaksonen, A., Raatikainen, T., Rautiainen, J., Vaattovaara, P., Ehn, M., Kulmala, M., Tomlinson, J. M., Collins, D. R., Cubison, M. J., E., Dunlea, J., Huffman, J. A., Onasch, T. B., Alfarra, M. R., Williams, P. I., Bower, K., Kondo, Y., Schneider, J., Drewnick, F., Borrmann, S., Weimer, S., Demerjian, K., Salcedo, D., Cottrell, L., Griffin, R., Takami, A., Miyoshi, T., Hatakeyama, S., Shimono, A., Sun, J. Y., Zhang, Y. M., Dzepina, K., Kimmel, J. R., Sueper, D., Jayne, J. T., Herndon, S. C., Trimborn, A. M., Williams, L. R., Wood, E. C., Middlebrook, A. M., Kolb, C. E., Baltensperger, U., and Worsnop, D. R.: Evolution of Organic Aerosols in the Atmosphere, Science, 326, 1525–1529, https://doi.org/10.1126/science.1180353, 2009.

Kahnert, M. and Kanngießer, F.: Optical properties of marine aerosol: modelling the transition from dry, irregularly shaped crystals to brine-coated, dissolving salt particles, Journal of Quantitative Spectroscopy and Radiative Transfer, 295, 108408, https://doi.org/10.1016/j.jqsrt.2022.108408, 2023.

Karl, M., Leck, C., Coz, E., and Heintzenberg, J.: Marine nanogels as a source of atmospheric nanoparticles in the high Arctic, Geophys. Res. Lett., 40, 3738–3743, https://doi.org/10.1002/grl.50661, 2013.

Kawamura, K. and Bikkina, S.: A review of dicarboxylic acids and related compounds in atmospheric aerosols: Molecular distributions, sources and transformation, Atmospheric Research, 170, 140–160, https://doi.org/10.1016/j.atmosres.2015.11.018, 2016.

Kirkby, J., Duplissy, J., Sengupta, K., Frege, C., Gordon, H., Williamson, C., Heinritzi, M., Simon, M., Yan, C., Almeida, J., Tröstl, J., Nieminen, T., Ortega, I. K., Wagner, R., Adamov, A., Amorim, A., Bernhammer, A.-K., Bianchi, F., Breitenlechner, M., Brilke, S., Chen, X., Craven, J., Dias, A., Ehrhart, S., Flagan, R. C., Franchin, A., Fuchs, C., Guida, R., Hakala, J., Hoyle, C. R., Jokinen, T., Junninen, H., Kangasluoma, J., Kim, J., Krapf, M., Kürten, A., Laaksonen, A., Lehtipalo, K., Makhmutov, V., Mathot, S., Molteni, U., Onnela, A., Peräkylä, O., Piel, F., Petäjä, T., Praplan, A. P., Pringle, K., Rap, A., Richards, N. A. D., Riipinen, I., Rissanen, M. P., Rondo, L., Sarnela, N., Schobesberger, S., Scott, C. E., Seinfeld, J. H., Sipilä, M., Steiner, G., Stozhkov, Y., Stratmann, F., Tomé, A., Virtanen, A., Vogel, A. L., Wagner, A. C., Wagner, P. E., Weingartner, E., Wimmer, D., Winkler, P. M., Ye, P., Zhang, X., Hansel, A., Dommen, J., Donahue, N. M., Worsnop, D. R., Baltensperger, U., Kulmala, M., Carslaw, K. S., and Curtius, J.: Ion-induced nucleation of pure biogenic particles, Nature, 533, 521–526, https://doi.org/10.1038/nature17953, 2016.

Kołodziejczyk, A., Pyrcz, P., Pobudkowska, A., Błaziak, K., and Szmigielski, R.: Physicochemical Properties of Pinic, Pinonic, Norpinic, and Norpinonic Acids as Relevant α-Pinene Oxidation Products, J. Phys. Chem. B, 123, 8261–8267, https://doi.org/10.1021/acs.jpcb.9b05211, 2019.

Koteska, D., Sanchez Garcia, S., Wagner-Döbler, I., and Schulz, S.: Identification of Volatiles of the Dinoflagellate Prorocentrum cordatum, Marine Drugs, 20, 371, https://doi.org/10.3390/md20060371, 2022.

Kroll, J. A., Frandsen, B. N., Kjaergaard, H. G., and Vaida, V.: Atmospheric Hydroxyl Radical Source: Reaction of Triplet SO_2 and Water, J. Phys. Chem. A, 122, 4465–4469, https://doi.org/10.1021/acs.jpca.8b03524, 2018.

Landwehr, S., Volpi, M., Haumann, F. A., Robinson, C. M., Thurnherr, I., Ferracci, V., Baccarini, A., Thomas, J., Gorodetskaya, I., Tatzelt, C., Henning, S., Modini, R. L., Forrer, H. J., Lin, Y., Cassar, N., Simó, R., Hassler, C., Moallemi, A., Fawcett, S. E., Harris, N., Airs, R., Derkani, M. H., Alberello, A., Toffoli, A., Chen, G., Rodríguez-Ros, P., Zamanillo, M., Cortés-Greus, P., Xue, L., Bolas, C. G., Leonard, K. C., Perez-Cruz, F., Walton, D., and Schmale, J.: Exploring the coupled ocean and atmosphere system with a data science approach applied to observations from the Antarctic Circumnavigation Expedition, Earth Syst. Dynam., 12, 1295–1369, https://doi.org/10.5194/esd-12-1295-2021, 2021.

Laskin, A., Laskin, J., and Nizkorodov, S. A.: Mass spectrometric approaches for chemical characterisation of atmospheric aerosols: critical review of the most recent advances, Environ. Chem., 9, 163, https://doi.org/10.1071/EN12052, 2012.

Lawler, M. J., Schill, G. P., Brock, C. A., Froyd, K. D., Williamson, C., Kupc, A., and Murphy, D. M.: Sea Spray Aerosol Over the Remote Oceans Has Low Organic Content, AGU Advances, 5, e2024AV001215, https://doi.org/10.1029/2024AV001215, 2024.

920   Lee, H. D., Morris, H. S., Laskina, O., Sultana, C. M., Lee, C., Jayarathne, T., Cox, J. L., Wang, X., Hasenecz, E. S., DeMott, P. J., Bertram, T. H., Cappa, C. D., Stone, E. A., Prather, K. A., Grassian, V. H., and Tivanski, A. V.: Organic Enrichment, Physical Phase State, and Surface Tension Depression of Nascent Core–Shell Sea Spray Aerosols during Two Phytoplankton Blooms, ACS Earth Space Chem., 4, 650–660, https://doi.org/10.1021/acsearthspacechem.0c00032, 2020.

925   Lehahn, Y., Koren, I., Schatz, D., Frada, M., Sheyn, U., Boss, E., Efrati, S., Rudich, Y., Trainic, M., Sharoni, S., Laber, C., DiTullio, G. R., Coolen, M. J. L., Martins, A. M., Van Mooy, B. A. S., Bidle, K. D., and Vardi, A.: Decoupling Physical from Biological Processes to Assess the Impact of Viruses on a Mesoscale Algal Bloom, Current Biology, 24, 2041–2046, https://doi.org/10.1016/j.cub.2014.07.046, 2014.

Lewis, S. L., Saliba, G., Russell, L. M., Quinn, P. K., Bates, T. S., and Behrenfeld, M. J.: Seasonal Differences
930   in Submicron Marine Aerosol Particle Organic Composition in the North Atlantic, Front. Mar. Sci., 8, 720208, https://doi.org/10.3389/fmars.2021.720208, 2021.

Li, Y., Bai, B., Dykema, J., Shin, N., Lambe, A. T., Chen, Q., Kuwata, M., Ng, N. L., Keutsch, F. N., and Liu, P.: Predicting Real Refractive Index of Organic Aerosols From Elemental Composition, Geophysical Research Letters, 50, e2023GL103446, https://doi.org/10.1029/2023GL103446, 2023.

935   Lin, C., Ceburnis, D., Hellebust, S., Buckley, P., Wenger, J., Canonaco, F., Prévôt, A. S. H., Huang, R.-J., O'Dowd, C., and Ovadnevaite, J.: Characterization of Primary Organic Aerosol from Domestic Wood, Peat, and Coal Burning in Ireland, Environ. Sci. Technol., 51, 10624–10632, https://doi.org/10.1021/acs.est.7b01926, 2017.

Lin, C., Ceburnis, D., Huang, R.-J., Xu, W., Spohn, T., Martin, D., Buckley, P., Wenger, J., Hellebust, S.,
940   Rinaldi, M., Facchini, M. C., O'Dowd, C., and Ovadnevaite, J.: Wintertime aerosol dominated by solid-fuel-burning emissions across Ireland: insight into the spatial and chemical variation in submicron aerosol, Atmos. Chem. Phys., 19, 14091–14106, https://doi.org/10.5194/acp-19-14091-2019, 2019.

Liu, Y., Ma, C., and Sun, J.: Integrated FT-ICR MS and metabolome reveals diatom-derived organic matter by bacterial transformation under warming and acidification, iScience, 26, 106812,
945   https://doi.org/10.1016/j.isci.2023.106812, 2023.

Loh, A., Kim, D., An, J. G., Choi, N., and Yim, U. H.: Chemical characterization of sub-micron aerosols over the East Sea (Sea of Japan), Science of The Total Environment, 856, 159173, https://doi.org/10.1016/j.scitotenv.2022.159173, 2023.

Loh, A., Kim, D., An, J. G., Choi, N., and Yim, U. H.: Characteristics of sub-micron aerosols in the Yellow Sea
950   and its environmental implications, Marine Pollution Bulletin, 204, 116556, https://doi.org/10.1016/j.marpolbul.2024.116556, 2024.

Mallet, M. D., D'Anna, B., Même, A., Bove, M. C., Cassola, F., Pace, G., Desboeufs, K., Di Biagio, C., Doussin, J.-F., Maille, M., Massabò, D., Sciare, J., Zapf, P., Di Sarra, A. G., and Formenti, P.: Summertime surface PM_1 aerosol composition and size by source region at the Lampedusa island in
955   the central Mediterranean Sea, Atmos. Chem. Phys., 19, 11123–11142, https://doi.org/10.5194/acp-19-11123-2019, 2019.

Malloy, Q. G. J., Li Qi, Warren, B., Cocker Iii, D. R., Erupe, M. E., and Silva, P. J.: Secondary organic aerosol formation from primary aliphatic amines with NO_3 radical, Atmos. Chem. Phys., 9, 2051–2060, https://doi.org/10.5194/acp-9-2051-2009, 2009.

960   Mansour, K., Decesari, S., Facchini, M. C., Belosi, F., Paglione, M., Sandrini, S., Bellacicco, M., Marullo, S., Santoleri, R., Ovadnevaite, J., Ceburnis, D., O'Dowd, C., Roberts, G., Sanchez, K., and Rinaldi, M.: Linking Marine Biological Activity to Aerosol Chemical Composition and Cloud-Relevant Properties Over the North Atlantic Ocean, J. Geophys. Res. Atmos., 125, https://doi.org/10.1029/2019JD032246, 2020.

Mansour, K., Decesari, S., Ceburnis, D., Ovadnevaite, J., and Rinaldi, M.: Machine learning for prediction of
965   daily sea surface dimethylsulfide concentration and emission flux over the North Atlantic Ocean (1998–2021), Science of The Total Environment, 871, 162123, https://doi.org/10.1016/j.scitotenv.2023.162123, 2023.

Mansour, K., Decesari, S., Ceburnis, D., Ovadnevaite, J., Russell, L. M., Paglione, M., Poulain, L., Huang, S., O'Dowd, C., and Rinaldi, M.: IPB-MSA&SO$_4$: a daily 0.25° resolution dataset of in situ-produced biogenic methanesulfonic acid and sulfate over the North Atlantic during 1998–2022 based on machine learning, Earth Syst. Sci. Data, 16, 2717–2740, https://doi.org/10.5194/essd-16-2717-2024, 2024.

Marais, E. A., Jacob, D. J., Jimenez, J. L., Campuzano-Jost, P., Day, D. A., Hu, W., Krechmer, J., Zhu, L., Kim, P. S., Miller, C. C., Fisher, J. A., Travis, K., Yu, K., Hanisco, T. F., Wolfe, G. M., Arkinson, H. L., Pye, H. O. T., Froyd, K. D., Liao, J., and McNeill, V. F.: Aqueous-phase mechanism for secondary organic aerosol formation from isoprene: application to the southeast United States and co-benefit of SO$_2$ emission controls, Atmos. Chem. Phys., 16, 1603–1618, https://doi.org/10.5194/acp-16-1603-2016, 2016.

Markuszewski, P., Nilsson, E. D., Zinke, J., Mårtensson, E. M., Salter, M., Makuch, P., Kitowska, M., Niedźwiecka-Wróbel, I., Drozdowska, V., Lis, D., Petelski, T., Ferrero, L., and Piskozub, J.: Multi-year gradient measurements of sea spray fluxes over the Baltic Sea and the North Atlantic Ocean, https://doi.org/10.5194/egusphere-2024-1254, 3 June 2024.

Mayer, K. J., Wang, X., Santander, M. V., Mitts, B. A., Sauer, J. S., Sultana, C. M., Cappa, C. D., and Prather, K. A.: Secondary Marine Aerosol Plays a Dominant Role over Primary Sea Spray Aerosol in Cloud Formation, ACS Cent. Sci., 6, 2259–2266, https://doi.org/10.1021/acscentsci.0c00793, 2020.

Maykut, N. N., Lewtas, J., Kim, E., and Larson, T. V.: Source Apportionment of PM$_{2.5}$ at an Urban IMPROVE Site in Seattle, Washington, Environ. Sci. Technol., 37, 5135–5142, https://doi.org/10.1021/es030370y, 2003.

McNeill, V. F.: Aqueous Organic Chemistry in the Atmosphere: Sources and Chemical Processing of Organic Aerosols, Environ. Sci. Technol., 49, 1237–1244, https://doi.org/10.1021/es5043707, 2015.

Meador, T. B., Goldenstein, N. I., Gogou, A., Herut, B., Psarra, S., Tsagaraki, T. M., and Hinrichs, K.-U.: Planktonic Lipidome Responses to Aeolian Dust Input in Low-Biomass Oligotrophic Marine Mesocosms, Front. Mar. Sci., 4, 113, https://doi.org/10.3389/fmars.2017.00113, 2017.

Middlebrook, A. M., Bahreini, R., Jimenez, J. L., and Canagaratna, M. R.: Evaluation of Composition-Dependent Collection Efficiencies for the Aerodyne Aerosol Mass Spectrometer using Field Data, Aerosol Science and Technology, 46, 258–271, https://doi.org/10.1080/02786826.2011.620041, 2012.

Miyazaki, Y., Sawano, M., and Kawamura, K.: Low-molecular-weight hydroxyacids in marine atmospheric aerosol: evidence of a marine microbial origin, Biogeosciences, 11, 4407–4414, https://doi.org/10.5194/bg-11-4407-2014, 2014.

Mohr, C., DeCarlo, P. F., Heringa, M. F., Chirico, R., Slowik, J. G., Richter, R., Reche, C., Alastuey, A., Querol, X., Seco, R., Peñuelas, J., Jiménez, J. L., Crippa, M., Zimmermann, R., Baltensperger, U., and Prévôt, A. S. H.: Identification and quantification of organic aerosol from cooking and other sources in Barcelona using aerosol mass spectrometer data, Atmos. Chem. Phys., 12, 1649–1665, https://doi.org/10.5194/acp-12-1649-2012, 2012.

Moschos, V., Dzepina, K., Bhattu, D., Lamkaddam, H., Casotto, R., Daellenbach, K. R., Canonaco, F., Rai, P., Aas, W., Becagli, S., Calzolai, G., Eleftheriadis, K., Moffett, C. E., Schnelle-Kreis, J., Severi, M., Sharma, S., Skov, H., Vestenius, M., Zhang, W., Hakola, H., Hellén, H., Huang, L., Jaffrezo, J.-L., Massling, A., Nøjgaard, J. K., Petäjä, T., Popovicheva, O., Sheesley, R. J., Traversi, R., Yttri, K. E., Schmale, J., Prévôt, A. S. H., Baltensperger, U., and El Haddad, I.: Equal abundance of summertime natural and wintertime anthropogenic Arctic organic aerosols, Nat. Geosci., https://doi.org/10.1038/s41561-021-00891-1, 2022.

Mungall, E. L., Wong, J. P. S., and Abbatt, J. P. D.: Heterogeneous Oxidation of Particulate Methanesulfonic Acid by the Hydroxyl Radical: Kinetics and Atmospheric Implications, ACS Earth Space Chem., 2, 48–55, https://doi.org/10.1021/acsearthspacechem.7b00114, 2018.

Mutshinda, C. M., Finkel, Z. V., and Irwin, A. J.: Large shifts in diatom and dinoflagellate biomass in the North Atlantic over six decades, https://doi.org/10.1101/2024.07.02.601152, 4 July 2024.

Narayanaswamy, B. E., Renaud, P. E., Duineveld, G. C. A., Berge, J., Lavaleye, M. S. S., Reiss, H., and Brattegard, T.: Biodiversity Trends along the Western European Margin, PLoS ONE, 5, e14295, https://doi.org/10.1371/journal.pone.0014295, 2010.

1015   Nault, B. A., Croteau, P., Jayne, J., Williams, A., Williams, L., Worsnop, D., Katz, E. F., DeCarlo, P. F., and Canagaratna, M.: Laboratory evaluation of organic aerosol relative ionization efficiencies in the aerodyne aerosol mass spectrometer and aerosol chemical speciation monitor, Aerosol Science and Technology, 57, 981–997, https://doi.org/10.1080/02786826.2023.2223249, 2023.

Ng, N. L., Canagaratna, M. R., Jimenez, J. L., Chhabra, P. S., Seinfeld, J. H., and Worsnop, D. R.: Changes in
1020   organic aerosol composition with aging inferred from aerosol mass spectra, Atmospheric Chemistry and Physics, 11, 6465–6474, https://doi.org/10.5194/acp-11-6465-2011, 2011.

Nielsen, I. E., Skov, H., Massling, A., Eriksson, A. C., Dall'Osto, M., Junninen, H., Sarnela, N., Lange, R., Collier, S., Zhang, Q., Cappa, C. D., and Nøjgaard, J. K.: Biogenic and anthropogenic sources of aerosols at the High Arctic site Villum Research Station, Atmos. Chem. Phys., 19, 10239–10256, https://doi.org/10.5194/acp-
1025   19-10239-2019, 2019.

Nøjgaard, J. K., Peker, L., Pernov, J. B., Johnson, M. S., Bossi, R., Massling, A., Lange, R., Nielsen, I. E., Prevot, A. S. H., Eriksson, A. C., Canonaco, F., and Skov, H.: A local marine source of atmospheric particles in the High Arctic, Atmospheric Environment, 285, 119241, https://doi.org/10.1016/j.atmosenv.2022.119241, 2022.

1030   Nursanto, F. R., Meinen, R., Holzinger, R., Krol, M. C., Liu, X., Dusek, U., Henzing, B., and Fry, J. L.: What chemical species are responsible for new particle formation and growth in the Netherlands? A hybrid positive matrix factorization (PMF) analysis using aerosol composition (ACSM) and size (SMPS), Aerosols/Field Measurements/Troposphere/Chemistry (chemical composition and reactions), https://doi.org/10.5194/egusphere-2023-554, 2023.

1035   O'Dowd, C., Ceburnis, D., Ovadnevaite, J., Vaishya, A., Rinaldi, M., and Facchini, M. C.: Do anthropogenic, continental or coastal aerosol sources impact on a marine aerosol signature at Mace Head?, Atmos. Chem. Phys., 14, 10687–10704, https://doi.org/10.5194/acp-14-10687-2014, 2014.

O'Dowd, C., Ceburnis, D., Ovadnevaite, J., Bialek, J., Stengel, D. B., Zacharias, M., Nitschke, U., Connan, S., Rinaldi, M., Fuzzi, S., Decesari, S., Cristina Facchini, M., Marullo, S., Santoleri, R., Dell'Anno, A., Corinaldesi,
1040   C., Tangherlini, M., and Danovaro, R.: Connecting marine productivity to sea-spray via nanoscale biological processes: Phytoplankton Dance or Death Disco?, Sci Rep, 5, 14883, https://doi.org/10.1038/srep14883, 2015.

O'Dowd, C. D., Facchini, M. C., Cavalli, F., Ceburnis, D., Mircea, M., Decesari, S., Fuzzi, S., Yoon, Y. J., and Putaud, J.-P.: Biogenically driven organic contribution to marine aerosol, Nature, 431, 676–680, https://doi.org/10.1038/nature02959, 2004.

1045   Ovadnevaite, J., O'Dowd, C., Dall'Osto, M., Ceburnis, D., Worsnop, D. R., and Berresheim, H.: Detecting high contributions of primary organic matter to marine aerosol: A case study: PRIMARY ORGANIC MARINE AEROSOL, Geophys. Res. Lett., 38, n/a-n/a, https://doi.org/10.1029/2010GL046083, 2011a.

Ovadnevaite, J., Ceburnis, D., Martucci, G., Bialek, J., Monahan, C., Rinaldi, M., Facchini, M. C., Berresheim, H., Worsnop, D. R., and O'Dowd, C.: Primary marine organic aerosol: A dichotomy of low hygroscopicity and
1050   high CCN activity: MARINE AEROSOL-CLOUD INTERACTIONS, Geophys. Res. Lett., 38, n/a-n/a, https://doi.org/10.1029/2011GL048869, 2011b.

Ovadnevaite, J., Ceburnis, D., Canagaratna, M., Berresheim, H., Bialek, J., Martucci, G., Worsnop, D. R., and O'Dowd, C.: On the effect of wind speed on submicron sea salt mass concentrations and source fluxes: EFFECT OF WIND SPEED ON SEA SALT, J. Geophys. Res., 117, n/a-n/a, https://doi.org/10.1029/2011JD017379,
1055   2012.

Ovadnevaite, J., Manders, A., de Leeuw, G., Ceburnis, D., Monahan, C., Partanen, A.-I., Korhonen, H., and O'Dowd, C. D.: A sea spray aerosol flux parameterization encapsulating wave state, Atmos. Chem. Phys., 14, 1837–1852, https://doi.org/10.5194/acp-14-1837-2014, 2014a.

1060   Ovadnevaite, J., Ceburnis, D., Leinert, S., Dall'Osto, M., Canagaratna, M., O'Doherty, S., Berresheim, H., and O'Dowd, C.: Submicron NE Atlantic marine aerosol chemical composition and abundance: Seasonal trends and air mass categorization: Seasonal Trends of Marine Aerosol, J. Geophys. Res. Atmos., 119, 11,850-11,863, https://doi.org/10.1002/2013JD021330, 2014b.

Ovadnevaite, J., Zuend, A., Laaksonen, A., Sanchez, K. J., Roberts, G., Ceburnis, D., Decesari, S., Rinaldi, M., Hodas, N., Facchini, M. C., Seinfeld, J. H., and O' Dowd, C.: Surface tension prevails over solute effect in
1065   organic-influenced cloud droplet activation, Nature, 546, 637–641, https://doi.org/10.1038/nature22806, 2017.

Oziel, L., Baudena, A., Ardyna, M., Massicotte, P., Randelhoff, A., Sallée, J.-B., Ingvaldsen, R. B., Devred, E., and Babin, M.: Faster Atlantic currents drive poleward expansion of temperate phytoplankton in the Arctic Ocean, Nat Commun, 11, 1705, https://doi.org/10.1038/s41467-020-15485-5, 2020.

Paatero, P.: The Multilinear Engine—A Table-Driven, Least Squares Program for Solving Multilinear Problems,
1070   Including the n -Way Parallel Factor Analysis Model, Journal of Computational and Graphical Statistics, 8, 854–888, https://doi.org/10.1080/10618600.1999.10474853, 1999.

Paatero, P. and Tapper, U.: Positive matrix factorization: A non-negative factor model with optimal utilization of error estimates of data values, Environmetrics, 5, 111–126, https://doi.org/10.1002/env.3170050203, 1994.

Paglione, M., Beddows, D. C. S., Jones, A., Lachlan-Cope, T., Rinaldi, M., Decesari, S., Manarini, F., Russo,
1075   M., Mansour, K., Harrison, R. M., Mazzanti, A., Tagliavini, E., and Dall'Osto, M.: Simultaneous organic aerosol source apportionment at two Antarctic sites reveals large-scale and ecoregion-specific components, Atmos. Chem. Phys., 24, 6305–6322, https://doi.org/10.5194/acp-24-6305-2024, 2024.

Park, J., Jang, J., Yoon, Y. J., Kang, S., Kang, H., Park, K., Cho, K. H., Kim, J.-H., Dall'Osto, M., and Lee, B. Y.: When river water meets seawater: Insights into primary marine aerosol production, Science of The Total
1080   Environment, 807, 150866, https://doi.org/10.1016/j.scitotenv.2021.150866, 2022.

Peltola, M., Rose, C., Trueblood, J. V., Gray, S., Harvey, M., and Sellegri, K.: Chemical precursors of new particle formation in coastal New Zealand, Aerosols/Field Measurements/Troposphere/Chemistry (chemical composition and reactions), https://doi.org/10.5194/acp-2022-307, 2022.

Pettersen, C., Henderson, S. A., Mattingly, K. S., Bennartz, R., and Breeden, M. L.: The Critical Role of Euro-
1085   Atlantic Blocking in Promoting Snowfall in Central Greenland, JGR Atmospheres, 127, e2021JD035776, https://doi.org/10.1029/2021JD035776, 2022.

van Pinxteren, M., Robinson, T.-B., Zeppenfeld, S., Gong, X., Bahlmann, E., Fomba, K. W., Triesch, N., Stratmann, F., Wurl, O., Engel, A., Wex, H., and Herrmann, H.: High number concentrations of transparent exopolymer particles in ambient aerosol particles and cloud water – a case study at the tropical Atlantic Ocean,
1090   Atmos. Chem. Phys., 22, 5725–5742, https://doi.org/10.5194/acp-22-5725-2022, 2022.

Preece, J. R., Mote, T. L., Cohen, J., Wachowicz, L. J., Knox, J. A., Tedesco, M., and Kooperman, G. J.: Summer atmospheric circulation over Greenland in response to Arctic amplification and diminished spring snow cover, Nat Commun, 14, 3759, https://doi.org/10.1038/s41467-023-39466-6, 2023.

Quinn, P. K., Coffman, D. J., Johnson, J. E., Upchurch, L. M., and Bates, T. S.: Small fraction of marine cloud
1095   condensation nuclei made up of sea spray aerosol, Nature Geosci, 10, 674–679, https://doi.org/10.1038/ngeo3003, 2017.

Radoman, N., Christiansen, S., Johansson, J., Hawkes, J., Bilde, M., Cousins, I. T., and Salter, M.: Probing the impact of a phytoplankton bloom on the chemistry of nascent sea spray aerosol using high-resolution mass spectrometry, Environ. Sci.: Atmos., 10.1039.D2EA00028H, https://doi.org/10.1039/D2EA00028H, 2022.

1100   Rahmstorf, S., Box, J. E., Feulner, G., Mann, M. E., Robinson, A., Rutherford, S., and Schaffernicht, E. J.: Exceptional twentieth-century slowdown in Atlantic Ocean overturning circulation, Nature Clim Change, 5, 475–480, https://doi.org/10.1038/nclimate2554, 2015.

Rapf, R. J., Dooley, M. R., Kappes, K., Perkins, R. J., and Vaida, V.: pH Dependence of the Aqueous Photochemistry of α-Keto Acids, J. Phys. Chem. A, 121, 8368–8379, https://doi.org/10.1021/acs.jpca.7b08192, 2017.

Rinaldi, M., Fuzzi, S., Decesari, S., Marullo, S., Santoleri, R., Provenzale, A., Von Hardenberg, J., Ceburnis, D., Vaishya, A., O'Dowd, C. D., and Facchini, M. C.: Is chlorophyll- *a* the best surrogate for organic matter enrichment in submicron primary marine aerosol?, JGR Atmospheres, 118, 4964–4973, https://doi.org/10.1002/jgrd.50417, 2013.

Rinaldi, M., Paglione, M., Decesari, S., Harrison, R. M., Beddows, D. C. S., Ovadnevaite, J., Ceburnis, D., O'Dowd, C. D., Simó, R., and Dall'Osto, M.: Contribution of Water-Soluble Organic Matter from Multiple Marine Geographic Eco-Regions to Aerosols around Antarctica, Environ. Sci. Technol., 54, 7807–7817, https://doi.org/10.1021/acs.est.0c00695, 2020.

Robinson, N. H., Hamilton, J. F., Allan, J. D., Langford, B., Oram, D. E., Chen, Q., Docherty, K., Farmer, D. K., Jimenez, J. L., Ward, M. W., Hewitt, C. N., Barley, M. H., Jenkin, M. E., Rickard, A. R., Martin, S. T., McFiggans, G., and Coe, H.: Evidence for a significant proportion of Secondary Organic Aerosol from isoprene above a maritime tropical forest, Atmos. Chem. Phys., 11, 1039–1050, https://doi.org/10.5194/acp-11-1039-2011, 2011.

Rosenfeld, D., Zhu, Y., Wang, M., Zheng, Y., Goren, T., and Yu, S.: Aerosol-driven droplet concentrations dominate coverage and water of oceanic low-level clouds, Science, 363, eaav0566, https://doi.org/10.1126/science.aav0566, 2019.

Rousseaux, C. S., Hirata, T., and Gregg, W. W.: Satellite views of global phytoplankton community distributions using an empirical algorithm and a numerical model, https://doi.org/10.5194/bgd-10-1083-2013, 24 January 2013.

Russell, L. M., Bahadur, R., and Ziemann, P. J.: Identifying organic aerosol sources by comparing functional group composition in chamber and atmospheric particles, Proc. Natl. Acad. Sci. U.S.A., 108, 3516–3521, https://doi.org/10.1073/pnas.1006461108, 2011.

S. Gerard Jennings, Christoph Kleefeld, Colin D. O'Dowd, Carsten Junker, T. Gerard Spain, Phillip O'Brien, Aodhaghan F. Roddy, and and Thomas C. O'Connor: Mace Head Atmospheric Research Station — characterization of aerosol radiative parameters, BOREAL ENVIRONMENT RESEARCH 8, 2003.

Saha, M. and Fink, P.: Algal volatiles – the overlooked chemical language of aquatic primary producers, Biological Reviews, 97, 2162–2173, https://doi.org/10.1111/brv.12887, 2022.

Saliba, G., Chen, C.-L., Lewis, S., Russell, L. M., Rivellini, L.-H., Lee, A. K. Y., Quinn, P. K., Bates, T. S., Haëntjens, N., Boss, E. S., Karp-Boss, L., Baetge, N., Carlson, C. A., and Behrenfeld, M. J.: Factors driving the seasonal and hourly variability of sea-spray aerosol number in the North Atlantic, Proc Natl Acad Sci USA, 116, 20309–20314, https://doi.org/10.1073/pnas.1907574116, 2019.

Sanchez, K. J., Zhang, B., Liu, H., Brown, M. D., Crosbie, E. C., Gallo, F., Hair, J. W., Hostetler, C. A., Jordan, C. E., Robinson, C. E., Scarino, A. J., Shingler, T. J., Shook, M. A., Thornhill, K. L., Wiggins, E. B., Winstead, E. L., Ziemba, L. D., Saliba, G., Lewis, S. L., Russell, L. M., Quinn, P. K., Bates, T. S., Porter, J., Bell, T. G., Gaube, P., Saltzman, E. S., Behrenfeld, M. J., and Moore, R. H.: North Atlantic Ocean SST-gradient-driven variations in aerosol and cloud evolution along Lagrangian cold-air outbreak trajectories, Atmos. Chem. Phys., 22, 2795–2815, https://doi.org/10.5194/acp-22-2795-2022, 2022.

Sanders, R. N. C., Jones, D. C., Josey, S. A., Sinha, B., and Forget, G.: Causes of the 2015 North Atlantic cold anomaly in a global state estimate, Ocean Sci., 18, 953–978, https://doi.org/10.5194/os-18-953-2022, 2022.

Schmale, J., Schneider, J., Nemitz, E., Tang, Y. S., Dragosits, U., Blackall, T. D., Trathan, P. N., Phillips, G. J., Sutton, M., and Braban, C. F.: Sub-Antarctic marine aerosol: dominant contributions from biogenic sources, Atmos. Chem. Phys., 13, 8669–8694, https://doi.org/10.5194/acp-13-8669-2013, 2013.

Schneider, J., Freutel, F., Zorn, S. R., Chen, Q., Farmer, D. K., Jimenez, J. L., Martin, S. T., Artaxo, P., Wiedensohler, A., and Borrmann, S.: Mass-spectrometric identification of primary biological particle markers

1150   and application to pristine submicron aerosol measurements in Amazonia, Atmos. Chem. Phys., 11, 11415–11429, https://doi.org/10.5194/acp-11-11415-2011, 2011.

Seidel, M., Vemulapalli, S. P. B., Mathieu, D., and Dittmar, T.: Marine Dissolved Organic Matter Shares Thousands of Molecular Formulae Yet Differs Structurally across Major Water Masses, Environ. Sci. Technol., 56, 3758–3769, https://doi.org/10.1021/acs.est.1c04566, 2022.

1155   Sellegri, K., Nicosia, A., Freney, E., Uitz, J., Thyssen, M., Grégori, G., Engel, A., Zäncker, B., Haëntjens, N., Mas, S., Picard, D., Saint-Macary, A., Peltola, M., Rose, C., Trueblood, J., Lefevre, D., D'Anna, B., Desboeufs, K., Meskhidze, N., Guieu, C., and Law, C. S.: Surface ocean microbiota determine cloud precursors, Sci Rep, 11, 281, https://doi.org/10.1038/s41598-020-78097-5, 2021.

Sellegri, K., Harvey, M., Peltola, M., Saint-Macary, A., Barthelmeß, T., Rocco, M., Moore, K. A., Cristi, A.,
1160   Peyrin, F., Barr, N., Labonnote, L., Marriner, A., McGregor, J., Safi, K., Deppeler, S., Archer, S., Dunne, E., Harnwell, J., Delanoe, J., Freney, E., Rose, C., Bazantay, C., Planche, C., Saiz-Lopez, A., Quintanilla-López, J. E., Lebrón-Aguilar, R., Rinaldi, M., Banson, S., Joseph, R., Lupascu, A., Jourdan, O., Mioche, G., Colomb, A., Olivares, G., Querel, R., McDonald, A., Plank, G., Bukosa, B., Dillon, W., Pelon, J., Baray, J.-L., Tridon, F., Donnadieu, F., Szczap, F., Engel, A., DeMott, P. J., and Law, C. S.: Sea2Cloud: From Biogenic Emission Fluxes
1165   to Cloud Properties in the Southwest Pacific, Bulletin of the American Meteorological Society, 104, E1017–E1043, https://doi.org/10.1175/BAMS-D-21-0063.1, 2023.

Semper, S., Våge, K., Pickart, R. S., Jónsson, S., and Valdimarsson, H.: Evolution and Transformation of the North Icelandic Irminger Current Along the North Iceland Shelf, JGR Oceans, 127, e2021JC017700, https://doi.org/10.1029/2021JC017700, 2022.

1170   Simon, H., Bhave, P. V., Swall, J. L., Frank, N. H., and Malm, W. C.: Determining the spatial and seasonal variability in OM/OC ratios across the US using multiple regression, Atmos. Chem. Phys., 11, 2933–2949, https://doi.org/10.5194/acp-11-2933-2011, 2011.

Slowik, J. G., Vlasenko, A., McGuire, M., Evans, G. J., and Abbatt, J. P. D.: Simultaneous factor analysis of organic particle and gas mass spectra: AMS and PTR-MS measurements at an urban site, Atmos. Chem. Phys.,
1175   10, 1969–1988, https://doi.org/10.5194/acp-10-1969-2010, 2010.

Stein, A. F., Draxler, R. R., Rolph, G. D., Stunder, B. J. B., Cohen, M. D., and Ngan, F.: NOAA's HYSPLIT Atmospheric Transport and Dispersion Modeling System, Bulletin of the American Meteorological Society, 96, 2059–2077, https://doi.org/10.1175/BAMS-D-14-00110.1, 2015.

Tong, Y., Qi, L., Stefenelli, G., Wang, D. S., Canonaco, F., Baltensperger, U., Prévôt, A. S. H., and Slowik, J.
1180   G.: Quantification of primary and secondary organic aerosol sources by combined factor analysis of extractive electrospray ionisation and aerosol mass spectrometer measurements (EESI-TOF and AMS), Aerosols/In Situ Measurement/Data Processing and Information Retrieval, https://doi.org/10.5194/amt-2022-78, 2022.

Ulbrich, I. M., Canagaratna, M. R., Zhang, Q., Worsnop, D. R., and Jimenez, J. L.: Interpretation of organic components from Positive Matrix Factorization of aerosol mass spectrometric data, Atmos. Chem. Phys., 9,
1185   2891–2918, https://doi.org/10.5194/acp-9-2891-2009, 2009.

Van Alstyne, K. and Houser, L.: Dimethylsulfide release during macroinvertebrate grazing and its role as an activated chemical defense, Mar. Ecol. Prog. Ser., 250, 175–181, https://doi.org/10.3354/meps250175, 2003.

Veron, F.: Ocean Spray, Annu. Rev. Fluid Mech., 47, 507–538, https://doi.org/10.1146/annurev-fluid-010814-014651, 2015.

1190   Villermaux, E., Wang, X., and Deike, L.: Bubbles spray aerosols: Certitudes and mysteries, PNAS Nexus, 1, pgac261, https://doi.org/10.1093/pnasnexus/pgac261, 2022.

Wang, Y., Zheng, X., Dong, X., Xi, B., Wu, P., Logan, T., and Yung, Y. L.: Impacts of long-range transport of aerosols on marine-boundary-layer clouds in the eastern North Atlantic, Atmos. Chem. Phys., 20, 14741–14755, https://doi.org/10.5194/acp-20-14741-2020, 2020.

1195 Willis, M. D., Köllner, F., Burkart, J., Bozem, H., Thomas, J. L., Schneider, J., Aliabadi, A. A., Hoor, P. M., Schulz, H., Herber, A. B., Leaitch, W. R., and Abbatt, J. P. D.: Evidence for marine biogenic influence on summertime Arctic aerosol, Geophys. Res. Lett., 44, 6460–6470, https://doi.org/10.1002/2017GL073359, 2017.

Willoughby, A., Wozniak, A., and Hatcher, P.: Detailed Source-Specific Molecular Composition of Ambient Aerosol Organic Matter Using Ultrahigh Resolution Mass Spectrometry and 1H NMR, Atmosphere, 7, 79,
1200 https://doi.org/10.3390/atmos7060079, 2016.

Wolf, K. K. E., Hoppe, C. J. M., Rehder, L., Schaum, E., John, U., and Rost, B.: Heatwave responses of Arctic phytoplankton communities are driven by combined impacts of warming and cooling, Sci. Adv., 10, eadl5904, https://doi.org/10.1126/sciadv.adl5904, 2024.

Xu, W., Lambe, A., Silva, P., Hu, W., Onasch, T., Williams, L., Croteau, P., Zhang, X., Renbaum-Wolff, L.,
1205 Fortner, E., Jimenez, J. L., Jayne, J., Worsnop, D., and Canagaratna, M.: Laboratory evaluation of species-dependent relative ionization efficiencies in the Aerodyne Aerosol Mass Spectrometer, null, 52, 626–641, https://doi.org/10.1080/02786826.2018.1439570, 2018.

Xu, W., Ovadnevaite, J., Fossum, K. N., Lin, C., Huang, R.-J., O'Dowd, C., and Ceburnis, D.: Aerosol hygroscopicity and its link to chemical composition in the coastal atmosphere of Mace Head: marine and
1210 continental air masses, Atmos. Chem. Phys., 20, 3777–3791, https://doi.org/10.5194/acp-20-3777-2020, 2020.

Xu, W., Fossum, K. N., Ovadnevaite, J., Lin, C., Huang, R.-J., O'Dowd, C., and Ceburnis, D.: The impact of aerosol size-dependent hygroscopicity and mixing state on the cloud condensation nuclei potential over the north-east Atlantic, Atmos. Chem. Phys., 21, 8655–8675, https://doi.org/10.5194/acp-21-8655-2021, 2021.

Yazdani, A., Dudani, N., Takahama, S., Bertrand, A., Prévôt, A. S. H., El Haddad, I., and Dillner, A. M.:
1215 Fragment ion–functional group relationships in organic aerosols using aerosol mass spectrometry and mid-infrared spectroscopy, Atmos. Meas. Tech., 15, 2857–2874, https://doi.org/10.5194/amt-15-2857-2022, 2022.

Zeppenfeld, S., Van Pinxteren, M., Hartmann, M., Zeising, M., Bracher, A., and Herrmann, H.: Marine Carbohydrates in Arctic Aerosol Particles and Fog – Diversity of Oceanic Sources and Atmospheric Transformations, Aerosols/Field Measurements/Troposphere/Chemistry (chemical composition and reactions),
1220 https://doi.org/10.5194/egusphere-2023-1607, 2023.

Zhang, Q., Jimenez, J. L., Canagaratna, M. R., Ulbrich, I. M., Ng, N. L., Worsnop, D. R., and Sun, Y.: Understanding atmospheric organic aerosols via factor analysis of aerosol mass spectrometry: a review, Anal Bioanal Chem, 401, 3045–3067, https://doi.org/10.1007/s00216-011-5355-y, 2011.

Zhao, Z., He, Q., Lu, Z., Zhao, Q., and Wang, J.: Analysis of Atmospheric CO2 and CO at Akedala Atmospheric
1225 Background Observation Station, a Regional Station in Northwestern China, IJERPH, 19, 6948, https://doi.org/10.3390/ijerph19116948, 2022.

Zheng, G., Wang, Y., Wood, R., Jensen, M. P., Kuang, C., McCoy, I. L., Matthews, A., Mei, F., Tomlinson, J. M., Shilling, J. E., Zawadowicz, M. A., Crosbie, E., Moore, R., Ziemba, L., Andreae, M. O., and Wang, J.: New particle formation in the remote marine boundary layer, Nat Commun, 12, 527, https://doi.org/10.1038/s41467-
1230 020-20773-1, 2021.